ETH
Eidgenössische Technische Hochschule Zürich
Swiss Federal Institute of Technology Zurich

Seminar for Applied Mathematics SAM

Multiple Traces Formulation and Semi-Implicit Scheme for Modeling Biological Cells under Electrical Stimulation

F. Henriquez and C. Jerez-Hanckes

Research Report No. 2017-23
May 2017

Seminar für Angewandte Mathematik
Eidgenössische Technische Hochschule
CH-8092 Zürich
Switzerland

Funding: This work was partially funded by Fondecyt Regular 1171491, Conicyt Anillo ACT1417 and Chile CORFO Engineering 2030 program through grant OPEN-UC 201603.

MULTIPLE TRACES FORMULATION AND SEMI-IMPLICIT SCHEME FOR MODELING BIOLOGICAL CELLS UNDER ELECTRICAL STIMULATION

FERNANDO HENRÍQUEZ AND CARLOS JEREZ-HANCKES

Abstract. We model the electrical behavior of several biological cells under external stimuli by extending and computationally improving the semi-implicit multiple traces formulation presented in (Henríquez *et al.*, Numerische Mathematik, 2016). Therein, the electric potential and current for a single cell are retrieved through the coupling of boundary integral operators and non-linear ordinary differential systems of equations. Yet, the low-order discretization scheme presented becomes impractical when accounting for interactions among multiple cells. In this note, we consider multi-cellular systems and show existence and uniqueness of the resulting non-linear evolution problem in finite time. Our main tools are analytic semigroup theory along with mapping properties of boundary integral operators in Sobolev spaces. Thanks to the smoothness of cellular shapes, solutions are highly regular at a given time. Hence, spectral spatial discretization can be employed, thereby largely reducing the number of unknowns. Time-space coupling is achieved via a semi-implicit time-stepping scheme shown to be stable and convergent. Numerical results in two dimensions validate our claims and match observed biological behavior for the Hodgkin-Huxley dynamical model.

This work was partially funded by Fondecyt Regular 1171491, Conicyt Anillo ACT1417 and Chile CORFO Engineering 2030 program through grant OPEN-UC 201603.

Contents

1. Introduction

Research and development in biomedical engineering as well as in biological sciences have greatly benefited from our ever-increasing ability to simulate complex cellular processes [27, 28, 34]. As computational resources and algorithmic efficiency improves, more realistic mathematical models can be used to better understand and enhance techniques such as localization and stimulation of peripheral nerves for anesthesia [9, 41, 7], cardiac defibrillation [46, 52], gene transfection [38, 13], membrane electro-permeabilization [50], and electro-chemotherapy of tumors [47, 18]. Yet, the intertwinement of multi-scale time-space phenomena, such as that which occurs when stimulating tissues containing several cells, remains a major challenge to the applied and computational mathematics community.

Cellular electrical behavior is dictated by the movement of ions through channels across the cell membrane. These channels are in turn composed of a large number of gates opening and closing randomly. Ion conduction occurs when all channel gates are open, an event whose probability depends on the voltage jump at the membrane. Several phenomenological descriptions of such random process have been offered [29]. The pioneering work of Hodgkin and Huxley [26] stands out as being the first model capable of modeling axon electrical activity and will constitute our model of choice without loss of generality. In order to obtain voltage differences between intra- and extra-cellular domains, Maxwell equations are employed. As bioelectric signals are significantly slower than electromagnetic ones, a quasi-static regime can be assumed that leads to the solving of Laplace equations in each subdomain. Hence, one seeks to couple a dynamic model taking place on cellular membranes with a static volumic one. The former is described by non-linear ordinary differential equations while the latter by partial differential equations. In the case of multiple cells, non-local electrostatic interactions need also to be duly accounted for.

Homogenization models present an alternative to simplify the above coupling [2, 1]. Here, the underlying idea hinges on reducing the heterogenous domain into an homogenous or effective medium. Hence, the methods rely on requiring a very large numbers of cells with respect to the physical scales of the quantities of interest simulated. Since we seek to understand the interactions among a large but finite number of closely interacting or packed cells, we opt for a different approach to homogenization though we cannot over stress the usefulness of such models in many biological simulations [17].

In [24], we modeled the electrical activity of one biological cell under external stimuli by coupling the local *Multiple Traces Formulation* (MTF) [25, 14, 15] with ionic dynamics at the membrane. Although the MTF was introduced to model heterogenous penetrable structures as in composite materials, it lends itself to solve scattering by multiple homogenous bodies. The gist of the MTF is to consider as unknowns Dirichlet and Neumann traces on either side of the cellular membrane. These traces must satisfy two requirements: Calderón identities per subdomain and transmission conditions. Hence, the volume problem is condensed to one posed over the cell boundary. To numerically couple it with our nonlinear dynamical model, in [24] we adopted a *time-stepping semi-implicit* Galerkin scheme for spatial low-order basis functions, with proven stability independent of space discretization and second order convergence. Our approach showed a considerable reduction of degrees of freedom when compared to previous methods as well as good agreement with experimental data. However, scalability of the method when considering multiple interacting cells is poor, as both the number of degrees of freedom and the conditioning numbers for the underlying matrices increase exponentially. Extending our previous work to address closely interacting or *packed* cells case constitutes the main goal of the present work.

As a first challenge, we are required to show that the resulting multi-cellular dynamic MTF system is well posed on the continuous level. Due to our boundary reduction, we must perform the analysis of Dirichlet-to-Neumann operators relating transmembrane voltages to currents given by the Hodgin-Huxley model. For this, we heavily rely on: (i) the mapping properties of boundary integral operators in fractional Sobolev spaces [16]; (ii) analytic group theory [40, 33, 36], and, (iii) linearity of the underlying system. The latter will allow us to define a suitable splitting of the sources of transmembrane currents on a given cell and analyze them individually. This result is valid in two and three dimensions and for a finite number of cells.

Computationally, one possible way to reduce the number of spatial unknowns relies on the observation that cellular shapes are smooth. Indeed, cells seek to maximize their area-to-volume ratio as a means to pass nutrients efficiently, which explains small cellular sizes and differentiable surfaces. Consequently, electric potentials will portray high regularity as long as the external stimulus is also sufficiently regular and that cells are touching each other. This scenario entails the possibility of replacing low-order basis by spectral

ones –Fourier polynomials in two dimensions or spherical harmonics in 3D–, eventually yielding exponential convergence rates, and consequently, greatly reducing the number of unknowns (*cf.* [23, 11, 31], [5, Section 6.5] or [44]). Still, cross interactions among cells potentials can foil computational performance regardless of the discretization basis employed.

Several schemes have been proposed to tackle multiple interactions [20, 19, 4, 6, 35]. The book by Martin [35] provides an extensive review of the main techniques in the subject. In [4], the two-dimensional time-harmonic acoustic multiple scattering problem at high-frequencies is solved by using series expansion. The method described hinges on the boundary decomposition technique introduced by Balabane [6] while the resolution and preconditioning of the underlying linear system is improved through the identification of particular matrix structures. In [20, 19, 21] the authors tackle Helmholtz and Maxwell multiple scattering problems by proposing different boundary integral equations, usually coupled with other techniques such as Balabane's boundary decomposition method [6] or the T–matrix method [54]. However, and to our knowledge, coupling such methods with nonlinear time dependent models as the one taking place in packed cells stimulation has not been yet performed. We believe the present work will open the path for such implementations.

This article is arranged as follows. In Section 2, we introduce necessary notation and tools to state the mathematical model problem for the interaction of multiple biological cells. Section 3 introduces boundary integral operators together with their main properties. In Section 4, the MTF is employed to recast the original volume problem as a problem solely posed on the cellular membranes. Existence and uniqueness of the boundary integral problem is presented in Section 5. The main tool in this case is analytic semigroup theory. Our numerical discretization scheme is described in Section 6, with stability and convergence analyses carried out in Sections 6.4 and 6.6, respectively. In Section 7, we show and discuss numerical results in the light of previous theoretical and experimental insights, and then conclude in Section 8.

2. Preliminaries and Model Volume Problem

2.1. **Notation.** Following [24], we set some of the recurring notation used throughout, with exceptions duly indicated. Let $D \subseteq \mathbb{R}^d$, with $d = 1, 2, 3$, be open. We denote by $\mathcal{C}^k(D)$ the space of k-times differentiable continuous functions over D with $k \in \mathbb{N}_0$. Also, let $L^p(D)$ be the standard class of functions with bounded L^p-norm over D. For $s \in \mathbb{R}$, $H^s(D)$ denotes standard Sobolev spaces with $H^0(D) \equiv L^2(D)$ [37, Chapter 3]. For D bounded, we will also use the notation $H^1(\Delta, D)$ for functions $u \in H^1(D)$ with $\Delta u \in L^2(D)$. For $s \geq 0$, we write $H^s_{\mathrm{loc}}(D)$ for the local Sobolev space of distributions whose restriction to every compact set $K \Subset D$ lies in $H^s(K)$. Similarly, we introduce the notation $H^s_{\mathrm{comp}}(D)$ for the space of compactly supported $H^s(D)$-functions in D, for $s \in \mathbb{R}$. For a Banach space V, $k \in \mathbb{N}_0$, functional spaces $\mathcal{C}^k([0,T];V)$ denote k-times continuous functions in t with bounded V-norm for all $t \in [0,T]$. An equivalent definition holds for $L^p([0,T];V)$ spaces with $p \in [1,\infty]$. $\mathcal{S}'(\mathbb{R}^d)$ denotes the Schwarz functional space of tempered distributions over $\mathbb{R}^d$. For Banach spaces X and Y, we also introduce the space of linear mappings $\mathcal{L}(X,Y)$ from X into Y.

Duality products are denoted by angular brackets, $\langle\cdot,\cdot\rangle$, while inner products by round brackets, $(\cdot,\cdot)$, both with subscripts accounting for the domain of defnition. Dual adjoint operators are denoted by prime superscripts, A'. Norms and semi-norms are denoted by $\|\cdot\|$, $|\cdot|$, respectively, with subscripts indicating the associated functional space. We use $\|\cdot\|_2$ to denote the euclidean norm in $\mathbb{R}^d$. Furthermore, time derivatives and vectors are denoted by the symbol ∂_t and by bold symbols, respectively.

2.2. **Problem Geometry.** Set $J \in \mathbb{N}$. Let $\Omega_j \Subset \mathbb{R}^d$, $d = 2, 3$ and $j = 1, \ldots, J$, be bounded Lipschitz –eventually smooth– subdomains each one with a connected boundary $\Gamma_j := \partial\Omega_j$ and complement $\Omega_j^c := \mathbb{R}^d \setminus \overline{\Omega}_j$. We assume that the set of subdomains is pairwise or mutually disjoint, i.e. $\overline{\Omega}_j \cap \overline{\Omega}_k = \emptyset$ whenever $j \neq k$, for $j, k = 1, \ldots, J$. The exterior domain to all subdomains, Ω_0, and its boundary Γ_0 are defined as

$$\Omega_0 := \mathbb{R}^d \setminus \bigcup_{j=1}^{J} \overline{\Omega}_j \quad \text{and} \quad \Gamma_0 := \bigcup_{j=1}^{J} \Gamma_j. \tag{2.1}$$

2.3. **Trace Operators and Multiple Trace Spaces.** Let us denote by $\boldsymbol{\nu}_j$ the outward unitary normal vector to a subdomain Γ_j, for $j = 1, \ldots, J$. Let γ^j be the interior trace operator acting from $H^s_{\mathrm{loc}}(\Omega_j)$ into

$H^{s-\frac{1}{2}}(\Gamma_j)$, for $\frac{1}{2} < s < \frac{3}{2}$ if Ω_j is Lipschitz, and if it is a $\mathcal{C}^k$-domain, for $\frac{1}{2} < s < k$ [45, Theorema 2.6.8 and 2.6.9]. For $u \in H^1_{\mathrm{loc}}(\Delta, \Omega_j)$, we introduce the *interior* Dirichlet and Neumann traces:

$$\gamma^j_{\mathrm{D}} u := \gamma^j u \quad \text{and} \quad \gamma^j_{\mathrm{N}} u := \gamma^j \left(\boldsymbol{\nu}_j \cdot \nabla u\right), \tag{2.2}$$

respectively. Analogously, we define *exterior* traces:

$$\gamma^{j,c}_{\mathrm{D}} u := \gamma^{j,c} u \quad \text{and} \quad \gamma^{j,c}_{\mathrm{N}} u := \gamma^{j,c} \left(\boldsymbol{\nu}_j \cdot \nabla u\right), \tag{2.3}$$

where $\gamma^{j,c}$ is the exterior trace operator mapping $H^s_{\mathrm{loc}}(\Omega_0)$ into $H^{s-\frac{1}{2}}(\Gamma_j)$ with conditions on s as those stated for interior traces. For a given subdomain boundary $\partial\Omega_j$, we set the product trace spaces per subdomain:

$$\mathbf{V}^s_j := H^{\frac{1}{2}+s}(\partial\Omega_j) \times H^{-\frac{1}{2}+s}(\partial\Omega_j),$$

with $|s| \leq \frac{1}{2}$ for bounded Lipschitz domain Ω_j or $s \in \mathbb{R}$ if Ω_j is bounded and $\mathcal{C}^\infty$. We identify $\mathbf{V}_j \equiv \mathbf{V}^0_j$. Also, for any $\boldsymbol{\varphi}$, $\boldsymbol{\xi}$ in $\mathbf{V}^s_j$, we define the *cross* or $\times$-duality product over Γ_j as (*cf.* [25, Section 2.2.1]):

$$\langle \boldsymbol{\varphi}, \boldsymbol{\xi} \rangle_{\times,j} := \langle \varphi_{\mathrm{D}}, \xi_{\mathrm{N}} \rangle_j + \langle \varphi_{\mathrm{N}}, \xi_{\mathrm{D}} \rangle_j . \tag{2.4}$$

Given an operator $\mathsf{B} : \mathbf{V}_k \to \mathbf{V}_j$, we can write

$$\mathsf{B} = \begin{pmatrix} \mathsf{B}_{\mathrm{DD}} & \mathsf{B}_{\mathrm{DN}} \\ \mathsf{B}_{\mathrm{ND}} & \mathsf{B}_{\mathrm{NN}} \end{pmatrix},$$

with obvious mapping properties, and obtain its $\times$-*dual adjoint* $\mathsf{B}^\dagger : \mathbf{V}_j \to \mathbf{V}_k$ as

$$\mathsf{B}^\dagger = \begin{pmatrix} \mathsf{B}'_{\mathrm{NN}} & \mathsf{B}'_{\mathrm{DN}} \\ \mathsf{B}'_{\mathrm{ND}} & \mathsf{B}'_{\mathrm{DD}} \end{pmatrix}, \tag{2.5}$$

since, for any $\boldsymbol{\lambda} \in \mathbf{V}_k$ and $\boldsymbol{\varphi} \in \mathbf{V}_j$, it holds

$$\begin{aligned} \langle \mathsf{B}\boldsymbol{\lambda}, \boldsymbol{\varphi} \rangle_{\times,j} &= \langle \mathsf{B}_{\mathrm{DD}} \lambda_{\mathrm{D}}, \varphi_{\mathrm{N}} \rangle_j + \langle \mathsf{B}_{\mathrm{DN}} \lambda_{\mathrm{N}}, \varphi_{\mathrm{N}} \rangle_j + \langle \mathsf{B}_{\mathrm{ND}} \lambda_{\mathrm{D}}, \varphi_{\mathrm{D}} \rangle_j + \langle \mathsf{B}_{\mathrm{NN}} \lambda_{\mathrm{N}}, \varphi_{\mathrm{D}} \rangle_j \\ &= \langle \lambda_{\mathrm{D}}, \mathsf{B}'_{\mathrm{DD}} \varphi_{\mathrm{N}} \rangle_k + \langle \lambda_{\mathrm{N}}, \mathsf{B}'_{\mathrm{DN}} \varphi_{\mathrm{N}} \rangle_k + \langle \lambda_{\mathrm{D}}, \mathsf{B}'_{\mathrm{ND}} \varphi_{\mathrm{D}} \rangle_k + \langle \lambda_{\mathrm{N}}, \mathsf{B}'_{\mathrm{NN}} \varphi_{\mathrm{D}} \rangle_k \\ &= \left\langle \boldsymbol{\lambda}, \mathsf{B}^\dagger \boldsymbol{\varphi} \right\rangle_{\times,k} . \end{aligned}$$

For shorthand, let us introduce the trace operators:

$$\boldsymbol{\gamma}^j u := \begin{pmatrix} \gamma^j_{\mathrm{D}} u \\ \gamma^j_{\mathrm{N}} u \end{pmatrix} : H^1_{\mathrm{loc}}(\Delta, \Omega_j) \to \mathbf{V}_j, \qquad \boldsymbol{\gamma}^{j,c} u := \begin{pmatrix} \gamma^{j,c}_{\mathrm{D}} u \\ \gamma^{j,c}_{\mathrm{N}} u \end{pmatrix} : H^1_{\mathrm{loc}}(\Delta, \Omega^c_j) \to \mathbf{V}_j. \tag{2.6}$$

Moreover, we define *trace and average jump operators* across Γ_j as follows: for $u \in H^1_{\mathrm{loc}}(\Delta, \Omega_j \cup \Omega^c_j)$, then

$$[\boldsymbol{\gamma} u]_j = \boldsymbol{\gamma}^{j,c} u - \boldsymbol{\gamma}^j u, \qquad \{\boldsymbol{\gamma} u\}_j = \frac{1}{2} \left(\boldsymbol{\gamma}^j u + \boldsymbol{\gamma}^{j,c} u\right), \tag{2.7}$$

respectively. Finally, we introduce the space $\mathbf{V}^{(2)}_j := \mathbf{V}_j \times \mathbf{V}_j$ as well as the *multiple traces space* $\mathbb{V}_J$ as the Cartesian product of interior and exterior trace spaces per subdomain boundary Γ_j:

$$\mathbb{V}_J := \prod_{j=1}^J \mathbf{V}^{(2)}_j .$$

These spaces[1] will be used in the MTF formulation of Section 3. For all Cartesian product spaces, inner and duality products as well as norms are sums of individual components with cross duality pairings. For example, for any $\boldsymbol{\lambda}^{(2)}_j = (\boldsymbol{\lambda}^c_j, \boldsymbol{\lambda}_j)^\top$ and $\boldsymbol{\varphi}^{(2)}_j = (\boldsymbol{\varphi}^c_j, \boldsymbol{\varphi}_j)^\top$ in $\mathbf{V}^{(2)}_j$, their dual product is defined as

$$\left\langle \boldsymbol{\lambda}^{(2)}_j, \boldsymbol{\varphi}^{(2)}_j \right\rangle_{\times,j} = \left\langle \boldsymbol{\lambda}^c_j, \boldsymbol{\varphi}^c_j \right\rangle_{\times,j} + \left\langle \boldsymbol{\lambda}_j, \boldsymbol{\varphi}_j \right\rangle_{\times,j}, \tag{2.8}$$

with norm

$$\begin{aligned} \left\| \boldsymbol{\varphi}^{(2)}_j \right\|_{\mathbf{V}^{(2)}_j} &:= \left\| \boldsymbol{\varphi}^c_j \right\|_{\mathbf{V}_j} + \left\| \boldsymbol{\varphi}_j \right\|_{\mathbf{V}_j} \\ &= \left\| \varphi^c_{\mathrm{D},j} \right\|_{H^{\frac{1}{2}}(\Gamma_j)} + \left\| \varphi^c_{\mathrm{N},j} \right\|_{H^{-\frac{1}{2}}(\Gamma_j)} + \left\| \varphi_{\mathrm{D},j} \right\|_{H^{\frac{1}{2}}(\Gamma_j)} + \left\| \varphi_{\mathrm{N},j} \right\|_{H^{-\frac{1}{2}}(\Gamma_j)} . \end{aligned} \tag{2.9}$$

[1]Here, exterior traces are ordered differently from the multiple traces space provided in [25, 14, 15] wherein all exterior traces are placed consecutively.

For $s \in \mathbb{R}$, let us also define

$$\mathbb{H}^s_J := H^s(\Gamma_1) \times \cdots \times H^s(\Gamma_J). \tag{2.10}$$

The dual space of $\mathbb{H}^s_J$ is $\mathbb{H}^{-s}_J$ with duality pairing given as follows. Let $\boldsymbol{u} = (u_1, u_2, \ldots, u_J) \in \mathbb{H}^s_J$ and $\boldsymbol{w} = (w_1, w_2, \ldots, w_J) \in \mathbb{H}^{-s}_J$, then the duality pairing is

$$\langle \boldsymbol{u}, \boldsymbol{w} \rangle_{\Gamma_0} = \sum_{j=1}^{J} \langle u_j, w_j \rangle_{\Gamma_j} \tag{2.11}$$

where $\langle \cdot, \cdot \rangle_{\Gamma_j}$ is the duality pairing defined over Γ_j. We set

$$\mathbb{L}^2_J \equiv \mathbb{H}^0_J = L^2(\Gamma_1) \times \cdots \times L^2(\Gamma_J). \tag{2.12}$$

2.4. **Continuous Volume Problem.** In what follows, we extend the continuous model presented in [24, Section 2] from a single cell to multiple ones. We assume the electric potential $u \in H^1_{\mathrm{loc}}(\Delta, \cup_{j=0}^{J} \Omega_j)$ to satisfy electrostatic equations in each subdomain Ω_j, i.e. for each $j = 0, \ldots, J$, if $u_j := u|_{\Omega_j}$, it must hold

$$-\operatorname{div} \sigma_j \nabla u_j = 0 \quad \text{in } \Omega_j,$$

where $\sigma_j \in L^\infty(\Omega_j)$ denotes the subdomain electrical conductivity [32, 53]. We further assume σ_j to be positive constants for all $j = 0, \ldots, J$.

We define the *transmembrane potential* v_j as the electric potential jump across the membrane Γ_j, from the inside to the outside, i.e. Ω_j to Ω_j^c. Furthermore, let us assume as given a potential field Φ_e, defined in Ω_0, such that $-\Delta \Phi_e = 0$ in Ω_0. This potential plays the role of an external source and in practice can be produced, for instance, by charged electrodes.

As in [24], we assume that the current membrane follows a time-dependent model. For $k = 1, \ldots, J$, the current i_k flowing across the membrane Γ_k is described as the sum of capacitive and ionic currents:

$$i_k = c_{m,k} \partial_t v_k + i_{\mathrm{ion},k} \quad \text{on } \Gamma_k, \tag{2.13}$$

where $c_{m,k}$ is the membrane capacitance per unit area and $i_{\mathrm{ion},k}$ stands for the ionic current of the k-th cell. Mathematically, a rigorous description of the ionic term is rather challenging, and thus, several models have been set forth based on experimental observations. Without loss of generality, we choose the so-called Hodgkin–Huxley (HH) model [26, 17] for the formulation presented below as well as for our numerical experiments (*cf.* [24]).

For a cellular membrane Γ_k, the HH model describes the ionic current $i_{\mathrm{ion},k}$ as a function of the transmembrane voltage v_k and a vector gate variable g_k. In the following, we write $i_{\mathrm{ion},k}(v_k, g_k)$ to explicitly state such dependence. Each vector gate variable g_k satisfies a system of ODEs in time over Γ_k, written as

$$\partial_t g_k = \mathcal{HH}_k(v_k, g_k) \quad \text{on } \Gamma_k, \tag{2.14}$$

along with adequate initial conditions.

The functions $i_{\mathrm{ion},k}(v_k, g_k)$, $\mathcal{HH}_k(v_k, g_k) : \mathbb{R} \times \mathbb{R} \to \mathbb{R}$ are analytic in both variables and one may extend their action to Sobolev spaces on the boundary Γ_k, for $k = 1, \ldots, J$ (*cf.* [43, Chapter 5] and [36, Lemma 5.4]).

Remark 2.1. The HH model actually incorporates three gates variables to describe the ionic current. For the sake of simplicity, throughout this work it is assumed the existence of solely one gate variable per biological cell, namely g_k. However, it is important to point out that in the computations presented in Section 7 the full HH model is employed.

The coupling between the membrane model, namely (2.13)–(2.14), and the potential field u relies on the membrane current:

$$i_k = -\sigma_k \gamma_{\mathrm{N}}^k u_k = -\sigma_0 \gamma_{\mathrm{N}}^{k,c} u_0 - \sigma_0 \gamma_{\mathrm{N}}^{k,c} \Phi_e, \quad \text{on } \Gamma_k, \tag{2.15}$$

for $k = 1, \ldots, J$. We can now state the volume formulation of the problem considered here as a generalization of [24, Problem 1]. We will assume $c_{m,k} \equiv c_m$ to simplify analysis.

Problem 2.2 (Continuous Volume Problem). Set a final time $T \in \mathbb{R}_+$ and initial conditions $v_j(0) = v_j^0$, $g_j(0) = g_j^0$. We seek suitably defined functions u_0, u_j, v_j and g_j, for $j = 1, \dots, J$, with support on Ω_0, Ω_j and Γ_j, respectively, such that, for all $t \in (0, T]$, it holds

$$-\Delta u_0 = 0 \quad \text{in } \Omega_0, \tag{2.16a}$$

$$-\Delta u_j = 0 \quad \text{in } \Omega_j, \quad j = 1, \dots, J, \tag{2.16b}$$

$$\gamma_{\mathrm{D}}^j u_j - \gamma_{\mathrm{D}}^{j,c} u_0 = v_j + \gamma_{\mathrm{D}}^{j,c} \Phi_e \quad \text{on } \Gamma_j, \quad j = 1, \dots, J, \tag{2.16c}$$

$$\sigma_j \gamma_{\mathrm{N}}^j u_j - \sigma_0 \gamma_{\mathrm{N}}^{j,c} u_0 = \sigma_0 \gamma_{\mathrm{N}}^{j,c} \Phi_e \quad \text{on } \Gamma_j, \quad j = 1, \dots, J, \tag{2.16d}$$

$$-\sigma_j \gamma_{\mathrm{N}}^j u_j = c_m \partial_t v_j + i_{\mathrm{ion},j}(v_j, g_j) \quad \text{on } \Gamma_j, \quad j = 1, \dots, J, \tag{2.16e}$$

$$\partial_t g_j = \mathcal{HH}(v_j, g_j) \quad \text{on } \Gamma_j, \quad j = 1, \dots, J, \tag{2.16f}$$

$$u_0 \text{ satisfies decay conditions at infinity.} \tag{2.16g}$$

More details regarding decay conditions at infinity can be found in [37, Theorem 8.9].

3. Multiple Traces Formulation

3.1. **Boundary Potentials and Integral Representation Formula.** For $d = 2, 3$, let $G(\boldsymbol{x}, \boldsymbol{y}) \in \mathcal{S}'(\mathbb{R}^d)$ be the fundamental solution to the Laplace operator in $\mathbb{R}^d$ (*cf.* [48, Chapter 5] or [45, Section 3.1]), whose expression is

$$G(\boldsymbol{x}, \boldsymbol{y}) = \begin{cases} \frac{1}{2\pi} \log \|\boldsymbol{x} - \boldsymbol{y}\|^{-1} & \boldsymbol{x} \neq \boldsymbol{y} \in \mathbb{R}^2, \\ \frac{1}{4\pi} \|\boldsymbol{x} - \boldsymbol{y}\|^{-1} & \boldsymbol{x} \neq \boldsymbol{y} \in \mathbb{R}^3. \end{cases} \tag{3.1}$$

For $s \in \mathbb{R}$, we define the *Newton potential* $\mathcal{N} : H^s_{\mathrm{comp}}(\mathbb{R}^d) \to H^{s+2}_{\mathrm{loc}}(\mathbb{R}^d)$ [45, Theorem 3.1.2] informally as

$$(\mathcal{N} f)(\boldsymbol{x}) := \int_{\mathbb{R}^d} G(\boldsymbol{x}, \boldsymbol{y}) f(\boldsymbol{y}) ds_{\boldsymbol{y}} \quad \forall\, \boldsymbol{x} \in \mathbb{R}^d, \tag{3.2}$$

with extension to Sobolev spaces based on density and duality arguments. Let us introduce the classic single and double layer potentials, $\mathcal{S}_j$ and $\mathcal{D}_j$, respectively, defined[2] over Γ_j as

$$\mathcal{S}_j := \mathcal{N} \circ \left(\gamma_{\mathrm{D}}^j\right)' \quad \text{and} \quad \mathcal{D}_j := \mathcal{N} \circ \left(\gamma_{\mathrm{N}}^j\right)', \tag{3.3}$$

for $j = 1, \dots, J$. We recall the following standard result:

Theorem 3.1 ([45], Theorema 3.1.16 & 3.1.12)**.** *For $j = 1, \dots, J$, the potentials $\mathcal{S}_j : H^{-\frac{1}{2}}(\Gamma_j) \to H^1_{\mathrm{loc}}\left(\mathbb{R}^d\right)$ and $\mathcal{D}_j : H^{\frac{1}{2}}(\Gamma_j) \to H^1_{\mathrm{loc}}\left(\mathbb{R}^d \setminus \Gamma_j\right)$ are continuous. Moreover, for $u_j \in H^1_{loc}\left(\Delta, \mathbb{R}^d \backslash \Gamma_j\right)$ satisfying the Laplace equation $-\Delta u_j = 0$ in $\mathbb{R}^d \backslash \Gamma_j$, the integral representation formula:*

$$u_j = -\mathcal{S}_j\left(\left[\gamma_N u_j\right]_j\right) + \mathcal{D}_j\left(\left[\gamma_D u_j\right]_j\right) \quad \text{in } \mathbb{R}^d \setminus \Gamma_j, \tag{3.4}$$

holds for all $j = 1, \dots, J$.

Functions satisfying (3.4) yield null trace jumps at subdomain boundaries Γ_k as long as $k \neq j$.

Theorem 3.2. *Let the function $u_0 \in H^1_{\mathrm{loc}}\left(\Delta, \mathbb{R}^d \setminus \Gamma_0\right)$ satisfy $-\Delta u_0 = 0$ in $\mathbb{R}^d \setminus \Gamma_0$. Then, the following integral representation formula holds*

$$u_0 = \sum_{j=1}^{J} -\mathcal{S}_j\left(\left[\gamma_N u_0\right]_j\right) + \mathcal{D}_j\left(\left[\gamma_D u_0\right]_j\right) \quad \text{in } \mathbb{R}^d \setminus \Gamma_0. \tag{3.5}$$

Proof. For $j = 1, \dots, J$, we define a family of functions $u_j \in H^1_{\mathrm{loc}}(\mathbb{R}^d \setminus \Gamma_j)$ solutions of the problem:

$$-\Delta u_j = 0 \quad \text{in } \mathbb{R}^d \backslash \Gamma_j, \tag{3.6a}$$

$$[\gamma u_j]_j = [\gamma u_0]_j \quad \text{on } \Gamma_j, \tag{3.6b}$$

[2]Though one should use L^2-adjoints instead of dual adjoints as in the Helmholtz case, for Laplace operators both definitions are equivalent as the kernel is symmetric and the inner and dual products are bilinear.

plus adequate decay conditions. The above problem has a unique solution $u_j \in H^1_{\rm loc}(\Delta, \mathbb{R}^d\backslash\overline{\Omega}_j)$ [45, Theorem 2.10.14]. Let us now sset

$$\hat{u}_0 := \sum_{j=1}^{J} u_j \quad \text{in } \mathbb{R}^d\backslash\Gamma_0. \tag{3.7}$$

By Theorem 3.1, we obtain

$$\hat{u}_0 = \sum_{j=1}^{J} -\mathcal{S}_j\left([\gamma_{\rm N} u_j]_j\right) + \mathcal{D}_j\left([\gamma_{\rm D} u_j]_j\right) \quad \text{in } \mathbb{R}^d. \tag{3.8}$$

Clearly, $-\Delta\hat{u}_0 = 0$ in $\mathbb{R}^d\backslash\Gamma_0$ and by construction $\hat{u}_0 \in H^1_{\rm loc}\left(\Delta, \mathbb{R}^d\backslash\Gamma_0\right)$. By trace jump continuity across Γ_ℓ for u_j, with $\ell \neq j$, it holds

$$[\boldsymbol{\gamma}\hat{u}_0]_\ell = \sum_{j=1}^{J} [\boldsymbol{\gamma} u_j]_\ell = [\boldsymbol{\gamma} u_\ell]_\ell = [\boldsymbol{\gamma} u_0]_\ell\,. \tag{3.9}$$

Hence, $\bar{u}_0 := \hat{u}_0 - u_0$ satisfies $-\Delta\bar{u}_0 = 0$ in $\mathbb{R}^d\backslash\Gamma_0$ with zero jump conditions over Γ_0. By uniqueness, $\bar{u}_0 \equiv 0$ leading to $\hat{u}_0 \equiv u_0$. Thus, the integral representation formula (3.5) holds for u_0. □

For simplicity, given $\boldsymbol{\lambda}_j = (\lambda^j_{\rm D}, \lambda^j_{\rm N})^\top \in \mathbf{V}_j$, we introduce the potential:

$$\Psi_j(\boldsymbol{\lambda}_j) := -\mathcal{S}_j\left(\lambda^j_{\rm N}\right) + \mathcal{D}_j\left(\lambda^j_{\rm D}\right). \tag{3.10}$$

3.2. **Boundary Integral Operators.** We introduce the standard Boundary Integral Operators (BIOs) over Γ_j [45]:

$$\mathsf{V}_j := \{\gamma_{\rm D} \circ \mathcal{S}_j\}_j : H^{-\frac{1}{2}}(\Gamma_j) \to H^{\frac{1}{2}}(\Gamma_j), \tag{3.11}$$

$$\mathsf{K}'_j := \{\gamma_{\rm N} \circ \mathcal{D}_j\}_j : H^{-\frac{1}{2}}(\Gamma_j) \to H^{-\frac{1}{2}}(\Gamma_j), \tag{3.12}$$

$$\mathsf{K}_j := \{\gamma_{\rm D} \circ \mathcal{S}_j\}_j : H^{\frac{1}{2}}(\Gamma_j) \to H^{\frac{1}{2}}(\Gamma_j), \tag{3.13}$$

$$\mathsf{W}_j := -\{\gamma_{\rm N} \circ \mathcal{D}_j\}_j : H^{\frac{1}{2}}(\Gamma_j) \to H^{-\frac{1}{2}}(\Gamma_j). \tag{3.14}$$

Theorem 3.3 ([48], Theorem 6.34)**.** *Let Γ_j be a bounded Lipschitz boundary in $\mathbb{R}^d$, $d = 2, 3$ for $j = 1, \ldots, J$ and $s \in \left[-\frac{1}{2}, \frac{1}{2}\right]$, the BIOs are linear and generate the following bounded mappings:*

$$\mathsf{V}_j : H^{-\frac{1}{2}+s}(\Gamma_j) \to H^{\frac{1}{2}+s}(\Gamma_j), \qquad \mathsf{K}_j : H^{\frac{1}{2}+s}(\Gamma_j) \to H^{\frac{1}{2}+s}(\Gamma_j),$$
$$\mathsf{K}'_j : H^{-\frac{1}{2}+s}(\Gamma_j) \to H^{-\frac{1}{2}+s}(\Gamma_j), \qquad \mathsf{W}_j : H^{\frac{1}{2}+s}(\Gamma_j) \to H^{-\frac{1}{2}+s}(\Gamma_j),$$

If Γ_j is a $\mathcal{C}^\infty$-boundary, the statement is valid for all $s \in \mathbb{R}$.

The traces of u_j, namely solutions of Problem 2.2, satisfy the following property:

$$\boldsymbol{\gamma}^j u = \begin{pmatrix} \gamma^j_{\rm D} u_j \\ \gamma^j_{\rm N} u_j \end{pmatrix} = \begin{pmatrix} \frac{1}{2}\mathsf{I} - \mathsf{K}_j & \mathsf{V}_j \\ \mathsf{W}_j & \frac{1}{2}\mathsf{I} + \mathsf{K}'_j \end{pmatrix} \begin{pmatrix} \gamma^j_{\rm D} u_j \\ \gamma^j_{\rm N} u_j \end{pmatrix} \text{ over } \Gamma_j, \quad j = 1, \ldots, J. \tag{3.15}$$

The block operator defined in (3.15), known as the *interior Calderón projector* and denoted by C_j, plays a key role in our boundary integral formulation. Consider the following decomposition:

$$\mathsf{C}_j = \frac{1}{2}\mathsf{I} + \mathsf{A}_j, \qquad \mathsf{A}_j := \begin{pmatrix} -\mathsf{K}_j & \mathsf{V}_j \\ \mathsf{W}_j & \mathsf{K}'_j \end{pmatrix}, \tag{3.16}$$

with $\mathsf{A}_j : \mathbf{V}^s_j \to \mathbf{V}^s_j$ continuously under the conditions given in Theorem 3.3. We also consider the *exterior* Calderón operator $\mathsf{C}^c_j = \frac{1}{2}\mathsf{I} - \mathsf{A}_j$.

Lemma 3.4 ([24], Lemma 2)**.** *For $j = 1, \ldots, J$, the operator $\mathsf{A}_j : \mathbf{V}_j \to \mathbf{V}_j$ is continuous and $\mathbf{V}_j$-coercive, i.e. it holds*

$$\langle \mathsf{A}_j\boldsymbol{\varphi}, \boldsymbol{\lambda}\rangle_{\times,j} \leq \alpha_j \left\|\boldsymbol{\varphi}\right\|_{\mathbf{V}_j} \left\|\boldsymbol{\lambda}\right\|_{\mathbf{V}_j}, \quad \forall\ \boldsymbol{\varphi}, \boldsymbol{\lambda} \in \mathbf{V}_j, \tag{3.17}$$

for a positive constant α_j, and there exists a compact operator $\mathsf{T}_{\mathsf{A}_j} : \mathbf{V}_j \to \mathbf{V}_j$ and a positive constant μ_j such that

$$\langle \mathsf{A}_j \boldsymbol{\varphi}, \boldsymbol{\varphi} \rangle_{\times,j} + \left\langle \mathsf{T}_{\mathsf{A}_j} \boldsymbol{\varphi}, \boldsymbol{\varphi} \right\rangle_{\times,j} \geq \mu_j \left\| \boldsymbol{\varphi} \right\|^2_{\mathbf{V}_j}, \quad \forall\, \boldsymbol{\varphi} \in \mathbf{V}_j. \tag{3.18}$$

3.3. **Multiple Traces Formulation.** For every $k = 1, \ldots, J$, Theorem 3.1 allows the use of the following integral representation for u_k satisfying Laplace's equation in Ω_k:

$$u_k = \mathcal{S}_k \left(\gamma_{\mathrm{N}}^k u_k \right) - \mathcal{D}_k \left(\gamma_{\mathrm{D}}^k u_k \right) \quad \text{in } \Omega_k. \tag{3.19}$$

Furthermore, if $\widetilde{u}_k$ denotes the extension of u_k by zero over Ω_k^c, i.e. $\widetilde{u}_k|_{\Omega_k^c} \equiv 0$, then (3.19) also holds over $\mathbb{R}^d \setminus \Gamma_k$. Taking interior traces yields

$$\boldsymbol{\gamma}^k u_k = \mathsf{C}_k \, \boldsymbol{\gamma}^k u_k \quad \text{on } \Gamma_k, \tag{3.20}$$

which is equivalent to

$$\frac{1}{2} \boldsymbol{\gamma}^k u_k = \mathsf{A}_k \, \boldsymbol{\gamma}^k u_k \quad \text{on } \Gamma_k. \tag{3.21}$$

On the other hand, let $u_0 \in H^1_{\mathrm{loc}}(\Delta, \Omega_0)$ satisfy $-\Delta u_0 = 0$ in Ω_0 and be such that its extension $\widetilde{u}_0$ by zero over Ω_k, i.e. $\widetilde{u}_0|_{\Omega_k} = 0$, for all $k = 1, \ldots, J$. Theorem 3.2 guarantees the representation:

$$u_0 = \sum_{j=1}^{J} -\mathcal{S}_j \left(\gamma_{\mathrm{N}}^{j,c} u_0 \right) + \mathcal{D}_j \left(\gamma_{\mathrm{D}}^{j,c} u_0 \right) \quad \text{in } \mathbb{R}^d \setminus \Gamma_0. \tag{3.22}$$

Taking exterior traces $\boldsymbol{\gamma}^{k,c}$ on Γ_k, we obtain

$$\boldsymbol{\gamma}^{k,c} u_0 = \mathsf{C}_k^{\mathsf{c}} \, \boldsymbol{\gamma}^{k,c} u_0 + \sum_{\substack{j=1 \\ j \neq k}}^{J} \mathsf{T}_{k,j} \, \boldsymbol{\gamma}^{j,c} u_0 \quad \text{on } \Gamma_k, \tag{3.23}$$

where

$$\mathsf{T}_{k,j} := \begin{pmatrix} \gamma_{\mathrm{D}}^{k,c} \circ \mathcal{D}_j & -\gamma_{\mathrm{D}}^{k,c} \circ \mathcal{S}_j \\ \gamma_{\mathrm{N}}^{k,c} \circ \mathcal{D}_j & -\gamma_{\mathrm{N}}^{k,c} \circ \mathcal{S}_j \end{pmatrix} : \mathbf{V}_j \to \mathbf{V}_k. \tag{3.24}$$

Equation (3.23) may be written as follows

$$\frac{1}{2} \boldsymbol{\gamma}^{k,c} u_0 = -\mathsf{A}_j \, \boldsymbol{\gamma}^{k,c} u_0 + \sum_{\substack{j=1 \\ j \neq k}}^{J} \mathsf{T}_{k,j} \, \boldsymbol{\gamma}^{j,c} u_0 \quad \text{on } \Gamma_k. \tag{3.25}$$

Let us set the excitation potential traces and transmembrane potential vectors:

$$\boldsymbol{\gamma}^{k,c} \Phi_e = (\gamma_{\mathrm{D}}^{k,c} \Phi_e, \gamma_{\mathrm{N}}^{k,c} \Phi_e)^\top \quad \text{and} \quad \mathcal{V}_k := (v_k, 0)^\top, \tag{3.26}$$

respectively. With the above observations, for all cell membranes Γ_k, $k = 1, \ldots, J$, transmission conditions (2.16c) and (2.16d), may be written as

$$\boldsymbol{\gamma}^k u_k - \mathsf{X}_k \boldsymbol{\gamma}^{k,c} u_0 = \mathsf{X}_k \left(\boldsymbol{\gamma}^{k,c} \Phi_e + \mathcal{V}_k \right) \quad \text{on } \Gamma_k, \tag{3.27}$$

wherein we have defined[3]

$$\mathsf{X}_k := \begin{pmatrix} \mathsf{I} & 0 \\ 0 & \frac{\sigma_0}{\sigma_k} \mathsf{I} \end{pmatrix} : \mathbf{V}_k \to \mathbf{V}_k. \tag{3.28}$$

Merging (3.21) together with (3.27) yields

$$\mathsf{A}_k \boldsymbol{\gamma}^k u_k - \frac{1}{2} \mathsf{X}_k \boldsymbol{\gamma}^{k,c} u_0 = \frac{1}{2} \mathsf{X}_k \left(\boldsymbol{\gamma}^{k,c} \Phi_e + \mathcal{V}_k \right), \tag{3.29}$$

whereas (3.23) in (3.27) renders

$$-\mathsf{A}_k \boldsymbol{\gamma}^{k,c} u_0 + \sum_{\substack{j=1 \\ j \neq k}}^{J} \mathsf{T}_{k,j} \boldsymbol{\gamma}^{j,c} u_0 - \frac{1}{2} \mathsf{X}_k^{-1} \boldsymbol{\gamma}^k u_k = -\frac{1}{2} \left(\boldsymbol{\gamma}^{k,c} \Phi_e + \mathcal{V}_k \right). \tag{3.30}$$

[3]Observe that this definition differs from that in [24, 25], as our work Neumann traces are directed along the outward normal vector, and consequently, there is no minus sign.

As shorthand, we denote the exterior and interior traces on a membrane Γ_j by $\boldsymbol{\lambda}_j^c := \boldsymbol{\gamma}^{j,c} u_0$ and $\boldsymbol{\lambda}_j := \boldsymbol{\gamma}^j u_j$, respectively. Moreover, since Neumann transmission conditions (2.16d) lead to ratios σ_j/σ_0, we introduce the notation:

$$\hat{\mathsf{A}}_j := \frac{\sigma_j}{\sigma_0}\mathsf{A}_j \quad \text{and} \quad \hat{\mathsf{X}}_j := \frac{\sigma_j}{\sigma_0}\mathsf{X}_j, \tag{3.31}$$

Define the block operator:

$$\mathsf{M}_j := \begin{pmatrix} \mathsf{A}_j & \frac{1}{2}\mathsf{X}_j^{-1} \\ -\frac{1}{2}\hat{\mathsf{X}}_j & \hat{\mathsf{A}}_j \end{pmatrix} : \mathbf{V}_j^{(2)} \to \mathbf{V}_j^{(2)}. \tag{3.32}$$

Lemma 3.5. *The operator M_j is continuous in $\mathbf{V}_j^{(2)}$, injective and coercive, i.e. it satisfies the Gårding-type inequality:*

$$\left\langle \mathsf{M}_j \boldsymbol{\lambda}_j^{(2)}, \boldsymbol{\lambda}_j^{(2)} \right\rangle_{\times,j} + \left\langle \mathsf{T}_{\mathsf{M}_j} \boldsymbol{\lambda}_j^{(2)}, \boldsymbol{\lambda}_j^{(2)} \right\rangle_{\times,j} \geq \mu_{\mathsf{M}_j} \left\| \boldsymbol{\lambda}_j^{(2)} \right\|^2_{\mathbf{V}_j^{(2)}} \quad \forall\, \boldsymbol{\lambda}_j^{(2)} \in \mathbf{V}_j^{(2)}, \tag{3.33}$$

where $\mu_{\mathsf{M}_j} > 0$, with duality products given as in (2.8).

Proof. Conductivities σ_j, $j = 1, \cdots, J$ are positive, yielding the quotient $\frac{\sigma_j}{\sigma_0}$ positive as well. Therefore, by Lemma 3.4, the operators A_j and $\hat{\mathsf{A}}_j$ are continuous and coercive with

$$\hat{\mathsf{T}}_{\mathsf{A}_j} := \frac{\sigma_j}{\sigma_0}\mathsf{T}_{\mathsf{A}_j} \quad \text{and} \quad \hat{\mu}_j := \mu_j \frac{\sigma_j}{\sigma_0}. \tag{3.34}$$

Coercivity of M_j follows as cross terms vanish yielding

$$\mathsf{T}_{\mathsf{M}_j} := \begin{pmatrix} \mathsf{T}_{\mathsf{A}_j} & 0 \\ 0 & \hat{\mathsf{T}}_{\mathsf{A}_j} \end{pmatrix} : \mathbf{V}_j^{(2)} \to \mathbf{V}_j^{(2)}, \quad \mu_{\mathsf{M}_j} := \mu_j \min\{1, \sigma_j/\sigma_0\}.$$

Injectivity is proved as in [25, Theorem 4]. □

Lemma 3.6. *For $j, k = 1, \ldots, J$ with $j \neq k$, the operators $\mathsf{T}_{k,j} : \mathbf{V}_j \to \mathbf{V}_k$ are continuously bounded for $|s| \leq \frac{1}{2}$. Furthermore, they are compact as mappings from $\mathbf{V}_j$ to $\mathbf{V}_k$.*

Proof. Since operators $\mathsf{T}_{k,j}$ for $j \neq k$ consist of four BIOs with continuous kernels, boundaries for integration and trace evaluation never coincide. Therefore, they map $\mathbf{V}_j \to \mathbf{V}_k^s$ for $s > 0$ and due to the compact embedding $\mathbf{V}_k^s \hookrightarrow \mathbf{V}_k$ [45, Theorem 2.5.5], the claim follows directly. □

Lemma 3.7. *The $\times$-adjoint $\mathsf{T}_{k,j}^\dagger = \mathsf{T}_{j,k}$ for $j, k = 1, \ldots, J$ and $j \neq k$.*

Proof. First, notice that $\mathcal{S}_j' = \gamma_{\mathrm{D}}^j \circ \mathcal{N}$ and $\mathcal{D}_j' = \gamma_{\mathrm{N}}^j \circ \mathcal{N}$, as $\mathcal{N}$ is self-adjoint. Then, by the definition of $\mathsf{T}_{j,k}$ (3.24) and using (2.5), we obtain

$$\mathsf{T}_{k,j}^\dagger = \begin{pmatrix} -\mathcal{S}_j' \circ \left(\gamma_{\mathrm{N}}^{k,c}\right)' & -\mathcal{S}_j' \circ \left(\gamma_{\mathrm{D}}^{k,c}\right)' \\ \mathcal{D}_j' \circ \left(\gamma_{\mathrm{N}}^{k,c}\right)' & \mathcal{D}_j' \circ \left(\gamma_{\mathrm{D}}^{k,c}\right)' \end{pmatrix} = \begin{pmatrix} -\gamma_{\mathrm{D}}^j \circ \mathcal{N} \circ \left(\gamma_{\mathrm{N}}^{k,c}\right)' & -\gamma_{\mathrm{D}}^j \circ \mathcal{N} \circ \left(\gamma_{\mathrm{D}}^{k,c}\right)' \\ \gamma_{\mathrm{N}}^j \circ \mathcal{N} \circ \left(\gamma_{\mathrm{N}}^{k,c}\right)' & \gamma_{\mathrm{N}}^j \circ \mathcal{N} \circ \left(\gamma_{\mathrm{D}}^{k,c}\right)' \end{pmatrix} \tag{3.35}$$

Observing that in this context $\gamma_{\mathrm{N}}^{j,c} = -\gamma_{\mathrm{N}}^j$ and that $\gamma_{\mathrm{D}}^{j,c} = \gamma_{\mathrm{D}}^j$, we conclude

$$\mathsf{T}_{k,j}^\dagger = = \begin{pmatrix} +\gamma_{\mathrm{D}}^{j,c} \circ \mathcal{N} \circ \left(\gamma_{\mathrm{N}}^k\right)' & -\gamma_{\mathrm{D}}^{j,c} \circ \mathcal{N} \circ \left(\gamma_{\mathrm{D}}^k\right)' \\ +\gamma_{\mathrm{N}}^{j,c} \circ \mathcal{N} \circ \left(\gamma_{\mathrm{N}}^k\right)' & -\gamma_{\mathrm{N}}^{j,c} \circ \mathcal{N} \circ \left(\gamma_{\mathrm{D}}^k\right)' \end{pmatrix} = \begin{pmatrix} \gamma_{\mathrm{D}}^{j,c} \circ \mathcal{D}_k & -\gamma_{\mathrm{D}}^{j,c} \circ \mathcal{S}_k \\ \gamma_{\mathrm{N}}^{j,c} \circ \mathcal{D}_k & -\gamma_{\mathrm{N}}^{j,c} \circ \mathcal{S}_k \end{pmatrix} = \mathsf{T}_{j,k} \tag{3.36}$$

as stated. □

Let us introduce the block operator:

$$\mathsf{Q}_{j,k} := \begin{pmatrix} -\mathsf{T}_{j,k} & 0 \\ 0 & 0 \end{pmatrix} : \mathbf{V}_k^{(2)} \to \mathbf{V}_j^{(2)}, \tag{3.37}$$

inheriting the same continuity and compactness properties of $\mathsf{T}_{j,k}$. Moreover, it also holds $\mathsf{Q}_{j,k}^\dagger = \mathsf{Q}_{k,j}$. Then, we can write down the boundary integral problem we seek to solve:

Problem 3.8 (MTF for J Mutually Disjoint Subdomains). Find $\boldsymbol{\lambda} = (\boldsymbol{\lambda}_1^c, \boldsymbol{\lambda}_1, \ldots, \boldsymbol{\lambda}_J^c, \boldsymbol{\lambda}_J)^\top \in \mathbb{V}_J$ such that the following variational problem:

$$\mathsf{m}_J(\boldsymbol{\lambda}, \boldsymbol{\varphi}) := \langle \mathbf{M}_J \boldsymbol{\lambda}, \boldsymbol{\varphi} \rangle_\times = \langle \mathbf{f}_J, \boldsymbol{\varphi} \rangle_\times, \quad \text{for all } \boldsymbol{\varphi} \in \mathbb{V}_J, \tag{3.38}$$

is satisfied, with duality pairing defined as sums of cross-pairings (2.4). The block operator on the left-hand-side is defined using (3.32) and (3.37) as

$$\mathbf{M}_J := \begin{pmatrix} \mathsf{M}_1 & \mathsf{Q}_{1,2} & \cdots & \mathsf{Q}_{1,J} \\ \mathsf{Q}_{2,1} & \mathsf{M}_2 & \cdots & \mathsf{Q}_{2,J} \\ \vdots & \vdots & \ddots & \vdots \\ \mathsf{Q}_{J,1} & \mathsf{Q}_{J,2} & \cdots & \mathsf{M}_J \end{pmatrix} : \mathbb{V}_J \to \mathbb{V}_J, \tag{3.39}$$

with source term $\mathbf{f}_J$ given in terms of the following components:

$$\boldsymbol{\mathcal{V}} := (\mathcal{V}_1, \mathcal{V}_1, \ldots, \mathcal{V}_J, \mathcal{V}_J) \in \mathbb{V}_J, \tag{3.40}$$

$$\boldsymbol{\phi}_e := (\boldsymbol{\gamma}^{1,c}\Phi_e, \boldsymbol{\gamma}^{1,c}\Phi_e, \ldots, \boldsymbol{\gamma}^{J,c}\Phi_e, \boldsymbol{\gamma}^{J,c}\Phi_e) \in \mathbb{V}_J, \tag{3.41}$$

$$\mathsf{F}_j := \begin{pmatrix} \mathsf{I} & 0 \\ 0 & \hat{\mathsf{X}}_j \end{pmatrix} \in \mathbf{V}_j^{(2)} \to \mathbf{V}_j^{(2)}, \tag{3.42}$$

so that

$$\mathbf{f}_J(\mathcal{V}_1, \ldots, \mathcal{V}_J, \boldsymbol{\phi}_e) := \frac{1}{2}\mathrm{diag}\,(\mathsf{F}_1, \mathsf{F}_2, \ldots, \mathsf{F}_J)\,(\boldsymbol{\mathcal{V}} + \boldsymbol{\phi}_e) \in \mathbb{V}_J. \tag{3.43}$$

We now prove the well–posedness of Problem 3.8 as a consequence of the Fredholm alternative.

Proposition 3.9. *The operator $\mathbf{M}_J : \mathbb{V}_J \to \mathbb{V}_J$ is injective, namely Problem 3.8 admits at most one solution.*

Proof. The proof follows the same arguments as those presented in [25, Theorem 4], which we skip for the sake of brevity. □

Proposition 3.10. *Let Γ_j be Lipchitz boundaries for $j = 1, \ldots, J$. The bilinear form $\mathsf{m}_J : \mathbb{V}_J^s \times \mathbb{V}_J^s \to \mathbb{R}$ is continuously bounded for $|s| \leq \frac{1}{2}$, i.e. for a constant $\alpha_J(s) > 0$ there holds*

$$|\mathsf{m}_J(\boldsymbol{\lambda}, \boldsymbol{\varphi})| \leq \alpha_J(s)\, \|\boldsymbol{\lambda}\|_{\mathbb{V}_J^s}\, \|\boldsymbol{\varphi}\|_{\mathbb{V}_J^s}, \quad \forall\, \boldsymbol{\lambda}, \boldsymbol{\varphi} \in \mathbb{V}_J^s, \tag{3.44}$$

and it is $\mathbb{V}_J$–coercive, i.e. there exists another constant $\mu_{\mathsf{m}_J} > 0$ and $\mathbf{T}_J : \mathbb{V}_J \to \mathbb{V}_J$ compact such that

$$\mathsf{m}_J(\boldsymbol{\lambda}, \boldsymbol{\lambda}) + \langle \mathbf{T}_J \boldsymbol{\lambda}, \boldsymbol{\lambda} \rangle_\times \geq \mu_{\mathsf{m}_J}\, \|\boldsymbol{\varphi}\|_{\mathbb{V}_J}^2, \quad \forall\, \boldsymbol{\lambda} \in \mathbb{V}_J. \tag{3.45}$$

Proof. Splitting $\boldsymbol{\lambda}$ and $\boldsymbol{\varphi}$ into its J components in $\mathbf{V}_j^{(2)}$, for $j = 1, \ldots, J$, the bilinear form m_J can be cast as follows

$$\mathsf{m}_J(\boldsymbol{\lambda}, \boldsymbol{\varphi}) = \sum_{j=1}^{J} \left\langle \mathsf{M}_j \boldsymbol{\lambda}_j^{(2)}, \boldsymbol{\varphi}_j^{(2)} \right\rangle_{\times,j} + \sum_{j=1}^{J} \sum_{\substack{k=1 \\ k \neq j}}^{J} \left\langle \mathsf{Q}_{j,k} \boldsymbol{\lambda}_k^{(2)}, \boldsymbol{\varphi}_j^{(2)} \right\rangle_{\times,j}. \tag{3.46}$$

Continuity follows from Lemmae 3.5 and 3.6 whereas coercivity is derived by combining Lemmae 3.5 and compactness of $\mathsf{Q}_{j,k}$. Specifically, the operator $\mathbf{T}_J$ is given by

$$\mathbf{T}_J := \begin{pmatrix} \mathsf{T}_{\mathsf{M}_1} & -\mathsf{Q}_{1,2} & \cdots & -\mathsf{Q}_{1,J} \\ -\mathsf{Q}_{2,1} & \mathsf{T}_{\mathsf{M}_2} & \ddots & -\mathsf{Q}_{2,J} \\ \vdots & \ddots & \ddots & \vdots \\ -\mathsf{Q}_{J,1} & -\mathsf{Q}_{J,2} & \cdots & \mathsf{T}_{\mathsf{M}_J} \end{pmatrix}. \tag{3.47}$$

Therefore,

$$\mathsf{m}_J(\boldsymbol{\lambda}, \boldsymbol{\lambda}) + (\mathbf{T}_J \boldsymbol{\lambda}, \boldsymbol{\lambda})_\times \geq \min_{j=1,\ldots,J} \mu_{\mathsf{M}_j}\, \|\boldsymbol{\lambda}\|_{\mathbb{V}_J}^2 \tag{3.48}$$

with $\mu_{\mathsf{m}_J} := \min_{j=1,\ldots,J} \mu_{\mathsf{M}_j} > 0$. □

4. MTF for Several Biological Cells

In what follows, we explain how the MTF given in Problem 3.8 relates to the transmembrane current in the HH model for many cells. Hence, from this point onwards all currents and potentials are time-dependent quantities. Yet, for the sake of brevity we forgo momentarily to write down such dependence. The transmembrane current across a cell boundary Γ_j can be expressed as contributions originated by the exterior potential Φ_e, ion currents $i_{\text{ion},j}$ and potential jumps v_j and v_k present at the surrounding $J-1$ cells. Explicitly, if we consider the unknown trace vector $\boldsymbol{\lambda} \in \mathbb{V}_J$ in (3.38), and recall the current equation (2.15), we deduce

$$-2i_j = \sigma_j \lambda_{j,\mathrm{N}} + \sigma_0 \lambda^c_{j,\mathrm{N}} + \sigma_0 \gamma^{j,c}_{\mathrm{N}} \Phi_e, \quad \text{on } \Gamma_j, \quad \forall\, j = 1, \dots, J, \tag{4.1}$$

or, equivalently,

$$i_j = -\frac{1}{2} \begin{pmatrix} 0 & \sigma_0 & 0 & \sigma_j \end{pmatrix} \boldsymbol{\lambda}^{(2)}_j - \frac{1}{2} \sigma_0 \gamma^{j,c}_{\mathrm{N}} \Phi_e, \quad \text{on } \Gamma_j, \quad \forall\, j = 1, \dots, J. \tag{4.2}$$

By linearity of Problem 3.8, we consider contributions for each term in (4.2) by switching on each component in $\mathbf{f}_J$ (3.43) while setting to zero off all other sources. Recalling the definition of $\mathbf{f}_J$, we can write the linear combination:

$$\mathbf{f}_J\left(\mathcal{V}_1, \dots \mathcal{V}_J, \boldsymbol{\phi}_e\right) = \sum_{j=1}^{J} \mathbf{f}^j_J(\boldsymbol{\phi}_e) + \sum_{j=1}^{J} \mathbf{f}^j_J\left(v_j\right) \in \mathbb{V}_J, \tag{4.3}$$

with components:

$$\mathbf{f}^j_J(\boldsymbol{\phi}_e) := \frac{1}{2} \left(\mathbf{0}, \dots, \mathbf{0}, \begin{pmatrix} \boldsymbol{\gamma}^{j,c} \Phi_e \\ \hat{\mathsf{X}}_j \boldsymbol{\gamma}^{j,c} \Phi_e \end{pmatrix}, \mathbf{0}, \dots, \mathbf{0} \right) \in \mathbb{V}_J, \tag{4.4}$$

$$\mathbf{f}^j_J(v_j) := \frac{1}{2} \left(\mathbf{0}, \dots, \mathbf{0}, \begin{pmatrix} \mathcal{V}_j \\ \hat{\mathsf{X}}_j \mathcal{V}_j \end{pmatrix}, \dots, \mathbf{0} \right) \in \mathbb{V}_J, \tag{4.5}$$

as v_j appears in the term $\mathcal{V}_j$. Each term leads to a corresponding solution of the MTF system given by the application of $\mathbf{M}_J^{-1}$ onto each right-hand side (4.4) and (4.5). From the statement of Problem 3.8, we can easily derive from the j-th block equation:

$$\boldsymbol{\lambda}^{(2)}_j = \frac{1}{2} \mathsf{M}_j^{-1} \mathbf{f}^j_J(\boldsymbol{\phi}_e) + \frac{1}{2} \mathsf{M}_j^{-1} \mathbf{f}^j_J(v_j) - \mathsf{M}_j^{-1} \sum_{\substack{k=1 \\ k \neq j}}^{J} \mathsf{Q}_{j,k} \boldsymbol{\lambda}^{(2)}_k \in \mathbf{V}^{(2)}_j. \tag{4.6}$$

Let us adopt the notation $\boldsymbol{\lambda}^{(2)}_j(v_k, \boldsymbol{\phi}_e)$ to explicitly show the dependence on a particular source, e.g., $\boldsymbol{\lambda}^{(2)}_j(v_k, \mathbf{0})$ is the solution of the traces pair over the j-th axon solely due to the transmembrane potential v_k. Plugging solutions (4.6) into (4.2) yields the electric current decomposition:

$$i_j = i_j(\boldsymbol{\phi}_e) + i_j(v_j) + \sum_{\substack{k=1 \\ k \neq j}}^{J} i_j(v_k) \quad \text{on } \Gamma_j, \tag{4.7}$$

wherein

$$i_j(\boldsymbol{\phi}_e) := -\frac{1}{2} \sigma_0 \gamma^{j,c}_{\mathrm{N}} \Phi_e - \frac{1}{2} \begin{pmatrix} 0 & \sigma_0 & 0 & \sigma_j \end{pmatrix} \left[\frac{1}{2} \mathsf{M}_j^{-1} \mathbf{f}^j_J(\boldsymbol{\phi}_e) - \mathsf{M}_j^{-1} \sum_{\substack{k=1 \\ k \neq j}}^{J} \mathsf{Q}_{j,k} \boldsymbol{\lambda}^{(2)}_k(0, \boldsymbol{\phi}_e) \right], \tag{4.8}$$

$$i_j(v_j) := -\frac{1}{2} \begin{pmatrix} 0 & \sigma_0 & 0 & \sigma_j \end{pmatrix} \left[\frac{1}{2} \mathsf{M}_j^{-1} \mathbf{f}^j_J(v_j) - \mathsf{M}_j^{-1} \sum_{\substack{k=1 \\ k \neq j}}^{J} \mathsf{Q}_{j,k} \boldsymbol{\lambda}^{(2)}_k(v_j, \mathbf{0}) \right], \tag{4.9}$$

$$i_j(v_k) := +\frac{1}{2} \begin{pmatrix} 0 & \sigma_0 & 0 & \sigma_j \end{pmatrix} \mathsf{M}_j^{-1} \mathsf{Q}_{j,k} \boldsymbol{\lambda}^{(2)}_k(v_k, \mathbf{0}). \tag{4.10}$$

Recall each term represents the electric current generated by a given source. We start by obtaining the contribution $i_j(v_j)$ due to one transmembrane potential v_j, or equivalently, set the external potential traces

$\boldsymbol{\phi}_e$ as well as v_k, for all $k \neq j$, equal to zero. Hence, by defining the following maps:

$$\mathcal{J}_j(v_j) := \frac{1}{4\sigma_0} \begin{pmatrix} 0 & \sigma_0 & 0 & \sigma_j \end{pmatrix} \mathsf{M}_j^{-1} \begin{pmatrix} \sigma_0 \\ 0 \\ \sigma_j \\ 0 \end{pmatrix} v_j \ : \ H^{\frac{1}{2}}(\Gamma_j) \to H^{-\frac{1}{2}}(\Gamma_j), \tag{4.11}$$

$$\mathcal{J}_k(v_j) := \frac{1}{2} \begin{pmatrix} 0 & \sigma_0 & 0 & \sigma_j \end{pmatrix} \mathsf{M}_j^{-1} \mathsf{Q}_{j,k} \boldsymbol{\lambda}_k^{(2)}(v_j, \mathbf{0}) \ : H^{\frac{1}{2}}(\Gamma_j) \to H^{-\frac{1}{2}}(\Gamma_j), \quad k \neq j, \tag{4.12}$$

we can also write (4.9) as the sum of contributions:

$$i_j(v_j) = -\mathcal{J}_j(v_j) + \sum_{\substack{k=1 \\ k \neq j}}^{J} \mathcal{J}_k(v_j). \tag{4.13}$$

Lemma 4.1. *For $j = 1, \ldots, J$, the operators $\mathcal{J}_j : H^{\frac{1}{2}+s}(\Gamma_j) \to H^{-\frac{1}{2}+s}(\Gamma_j)$ defined in (4.11) are continuous for $s \in \mathbb{R}$. Moreover, they are $H^{\frac{1}{2}}(\Gamma_j)$-coercive, i.e. it holds*

$$\left\langle \left(\mathcal{J}_j + \mathsf{T}_{\mathcal{J}_j} \right) v, v \right\rangle_{\Gamma_j} \geq c_{\mathcal{J}_j} \left\| v \right\|^2_{H^{\frac{1}{2}}(\Gamma_j)}, \quad \text{for all } v \in H^{\frac{1}{2}}(\Gamma_j), \tag{4.14}$$

where $c_{\mathcal{J}_j}$ is a positive constant and $\mathsf{T}_{\mathcal{J}_j} : H^{\frac{1}{2}+s}(\Gamma_j) \to H^{-\frac{1}{2}+s}(\Gamma_j)$ is compact. Besides, the operator $\mathcal{J}_j$ is self-adjoint.

For $k = 1, \ldots, J$ with $k \neq j$, the operators $\mathcal{J}_k : H^{\frac{1}{2}+s}(\Gamma_j) \to H^{-\frac{1}{2}+s}(\Gamma_j)$, are continuous for $s \geq 0$ and, furthermore, compact.

Proof. Continuity of $\mathcal{J}_j$ and $\mathcal{J}_k$, for $k \neq j$, comes from the fact that both operators are by definition the composition of continuous operators (*cf.* Lemmae 3.5 and 3.6). In particular, the operator $\mathcal{J}_k$ is defined as the composition of continuous and a compact operator, therefore it is compact as well.

From Lemma 3.5, M_j is invertible. Let $\boldsymbol{\varphi}_j^{(2)} \in \mathbf{V}_j^{(2)}$, then it holds

$$\begin{aligned} \left\langle \mathsf{M}_j \boldsymbol{\varphi}_j^{(2)}, \boldsymbol{\varphi}_j^{(2)} \right\rangle_{\times,j} &= \left\langle \mathsf{M}_j \left(\mathsf{M}_j^{\dagger} \right)^{-1} \mathsf{M}_j^{\dagger} \boldsymbol{\varphi}_j^{(2)}, \boldsymbol{\varphi}_j^{(2)} \right\rangle_{\times,j} \\ &= \left\langle \left(\mathsf{M}_j^{\dagger} \right)^{-1} \mathsf{M}_j^{\dagger} \boldsymbol{\varphi}_j^{(2)}, \mathsf{M}_j^{\dagger} \boldsymbol{\varphi}_j^{(2)} \right\rangle_{\times,j}. \end{aligned} \tag{4.15}$$

By using (2.8) and (2.5) one can easily derive $\mathsf{M}_j^{\dagger} = -\mathsf{M}_j$. Then,

$$\begin{aligned} \left\langle \left(\mathsf{M}_j^{\dagger} \right)^{-1} \mathsf{M}_j^{\dagger} \boldsymbol{\varphi}_j^{(2)}, \mathsf{M}_j^{\dagger} \boldsymbol{\varphi}_j^{(2)} \right\rangle_{\times,j} &= - \left\langle \mathsf{M}_j^{-1} \mathsf{M}_j^{\dagger} \boldsymbol{\varphi}_j^{(2)}, \mathsf{M}_j^{\dagger} \boldsymbol{\varphi}_j^{(2)} \right\rangle_{\times,j} \\ &= - \left\langle \mathsf{M}_j^{-1} \mathsf{M}_j^{\dagger} \boldsymbol{\varphi}_j^{(2)}, \mathsf{M}_j^{\dagger} \boldsymbol{\varphi}_j^{(2)} \right\rangle_{\times,j} \\ &= + \left\langle \mathsf{M}_j^{-1} \mathsf{M}_j^{\dagger} \boldsymbol{\varphi}_j^{(2)}, \mathsf{M}_j^{\dagger} \boldsymbol{\varphi}_j^{(2)} \right\rangle_{\times,j}. \end{aligned} \tag{4.16}$$

Defining $\boldsymbol{\lambda}_j^{(2)} = \mathsf{M}_j^{\dagger} \boldsymbol{\varphi}_j^{(2)} \in \mathbf{V}_j^{(2)}$ we have

$$\begin{aligned} \left\langle (\mathsf{M}_j + \mathsf{T}_{\mathsf{M}_j}) \boldsymbol{\varphi}_j^{(2)}, \boldsymbol{\varphi}_j^{(2)} \right\rangle_{\times,j} &= \left\langle \mathsf{M}_j^{-1} \boldsymbol{\lambda}_j^{(2)}, \boldsymbol{\lambda}_j^{(2)} \right\rangle_{\times,j} + \left\langle \mathsf{T}_{\mathsf{M}_j} \mathsf{M}_j^{-1} \boldsymbol{\lambda}_j^{(2)}, \mathsf{M}_j^{-1} \boldsymbol{\lambda}_j^{(2)} \right\rangle_{\times,j} \\ &= \left\langle \mathsf{M}_j^{-1} \boldsymbol{\lambda}_j^{(2)}, \boldsymbol{\lambda}_j^{(2)} \right\rangle_{\times,j} + \left\langle \left(\mathsf{M}_j^{-1} \right)^{\dagger} \mathsf{T}_{\mathsf{M}_j} \mathsf{M}_j^{-1} \boldsymbol{\lambda}_j^{(2)}, \boldsymbol{\lambda}_j^{(2)} \right\rangle_{\times,j} \\ &= \left\langle \mathsf{M}_j^{-1} \boldsymbol{\lambda}_j^{(2)}, \boldsymbol{\lambda}_j^{(2)} \right\rangle_{\times,j} + \left\langle \mathsf{M}_j^{-1} \mathsf{T}_{\mathsf{M}_j} \mathsf{M}_j^{-1} \boldsymbol{\lambda}_j^{(2)}, \boldsymbol{\lambda}_j^{(2)} \right\rangle_{\times,j} \\ &\geq \mu_{\mathsf{M}_j} \left\| \boldsymbol{\varphi}_j^{(2)} \right\|^2_{\mathbf{V}_j^{(2)}} \\ &\geq \frac{\mu_{\mathsf{M}_j}}{\left\| \mathsf{M}_j^{\dagger} \right\|_{\mathcal{L}\left(\mathbf{V}_j^{(2)}, \mathbf{V}_j^{(2)} \right)}} \left\| \boldsymbol{\lambda}_j^{(2)} \right\|^2_{\mathbf{V}_j^{(2)}} \end{aligned} \tag{4.17}$$

with μ_{M_j} given by Lemma 3.6. Therefore, if we define

$$\mu_{\mathsf{M}_j^{-1}} := \frac{\mu_{\mathsf{M}_j}}{\left\|\mathsf{M}_j^{\dagger}\right\|_{\mathcal{L}\left(\mathbf{V}_j^{(2)}\times\mathbf{V}_j^{(2)}\right)}} \qquad \text{and} \quad \mathsf{T}_{\mathsf{M}_j^{-1}} := \mathsf{M}_j^{-1}\mathsf{T}_{\mathsf{M}_j}\mathsf{M}_j^{-1} :\ \mathbf{V}_j^{(2)} \to \mathbf{V}_j^{(2)}, \tag{4.18}$$

the operator M_j^{-1} satisfies

$$\left\langle \left(\mathsf{M}_j^{-1} + \mathsf{T}_{\mathsf{M}_j^{-1}}\right)\boldsymbol{\lambda}_j^{(2)}, \boldsymbol{\lambda}_j^{(2)}\right\rangle_{\times,j} \geq \mu_{\mathsf{M}_j^{-1}} \left\|\boldsymbol{\lambda}_j^{(2)}\right\|^2_{\mathbf{V}_j^{(2)}}, \quad \forall\ \boldsymbol{\lambda}_j^{(2)} \in \mathbf{V}_j^{(2)}. \tag{4.19}$$

Clearly, the operator $\mathsf{T}_{\mathsf{M}_j^{-1}}$ is compact being the composition of compact and continuous operators. For the particular choice:

$$\boldsymbol{\lambda}_j^{(2)} = \begin{pmatrix} \sigma_0 \\ 0 \\ \sigma_j \\ 0 \end{pmatrix} v_j \tag{4.20}$$

where $v_j \in H^{\frac{1}{2}}(\Gamma_j)$, we have

$$\left\langle \begin{pmatrix} 0 & \sigma_0 & 0 & \sigma_j \end{pmatrix} \mathsf{M}_j^{-1} \begin{pmatrix} \sigma_0 \\ 0 \\ \sigma_j \\ 0 \end{pmatrix} v_j, v_j \right\rangle_{\Gamma_j} + \left\langle \begin{pmatrix} 0 & \sigma_0 & 0 & \sigma_j \end{pmatrix} \mathsf{T}_{\mathsf{M}_j^{-1}} \begin{pmatrix} \sigma_0 \\ 0 \\ \sigma_j \\ 0 \end{pmatrix} v_j, v_j \right\rangle_{\Gamma_j} \tag{4.21}$$

$$\geq \mu_{\mathsf{M}_j^{-1}} \left\| \begin{pmatrix} \sigma_0 \\ 0 \\ \sigma_j \\ 0 \end{pmatrix} v_j \right\|^2_{\mathbf{V}_j^{(2)}} \tag{4.22}$$

$$\geq 4\mu_{\mathsf{M}_j^{-1}} \left\|v_j\right\|^2_{H^{\frac{1}{2}}(\Gamma_j)}. \tag{4.23}$$

Therefore, the operator $\mathcal{J}_j$ satisfies the following Gårding inequality:

$$\left\langle \left(\mathcal{J}_j + \mathsf{T}_{\mathcal{J}_j}\right) v_j, v_j\right\rangle_{\Gamma_j} \geq 4c_{\mathsf{M}_j^{-1}} \left\|v_j\right\|^2_{H^{\frac{1}{2}}(\Gamma_j)} \tag{4.24}$$

for all $v_j \in H^{\frac{1}{2}}(\Gamma_j)$ and wherein

$$\mathsf{T}_{\mathcal{J}_j} := \begin{pmatrix} 0 & \sigma_0 & 0 & \sigma_j \end{pmatrix} \mathsf{T}_{\mathsf{M}_j^{-1}} \begin{pmatrix} \sigma_0 \\ 0 \\ \sigma_j \\ 0 \end{pmatrix} :\ H^{\frac{1}{2}}(\Gamma_j) \to H^{-\frac{1}{2}}(\Gamma_j) \tag{4.25}$$

is a compact operator. □

Define $\boldsymbol{v} = (v_1, \dots v_J)^\top$ and $\boldsymbol{g} = (g_1, \dots, g_J)^\top$ and recall all quantities are time-dependent. Let $\underline{\mathcal{J}} : \mathbb{H}_J^{\frac{1}{2}+s} \to \mathbb{H}_J^{-\frac{1}{2}+s}$ for $s \in \mathbb{R}$ be the operator defined as

$$\underline{\mathcal{J}} := \operatorname{diag}\left(\mathcal{J}_1, \mathcal{J}_2, \dots, \mathcal{J}_J\right) - \begin{pmatrix} \mathcal{J}_{1,1} & \cdots & \mathcal{J}_{1,J} \\ \vdots & \ddots & \vdots \\ \mathcal{J}_{J,1} & \cdots & \mathcal{J}_{J,J} \end{pmatrix}. \tag{4.26}$$

Based on (4.8) and (2.13), we also set the following:

$$\boldsymbol{i}_{\phi_e} := \begin{pmatrix} i_1(\boldsymbol{\phi}_e) \\ \vdots \\ i_J(\boldsymbol{\phi}_e) \end{pmatrix} \quad \text{and} \quad \boldsymbol{i}_{\text{ion}}(\boldsymbol{v}, \boldsymbol{g}) := \begin{pmatrix} i_{\text{ion},1}(v_1, g_1) \\ \vdots \\ i_{\text{ion},J}(v_J, g_J) \end{pmatrix}. \tag{4.27}$$

For the HH model we define

$$\mathcal{HH}(\boldsymbol{v},\boldsymbol{g}) := \begin{pmatrix} \mathcal{HH}_1(v_1,g_1) \\ \vdots \\ \mathcal{HH}_J(v_J,g_J), \end{pmatrix} \tag{4.28}$$

where $\mathcal{HH}_k$ are as in (2.14) and Remark 2.1 applies.

With the above definitions we are now in position to set the continuous boundary problem we aim to solve.

Problem 4.2 (MTF for Packed Cells Problem). Let $s > \frac{3}{2}$, initial given data $\boldsymbol{v}_0 \in \mathbb{H}_J^{\frac{1}{2}+s}$, $\boldsymbol{g}_0 \in \mathbb{H}_J^{-\frac{1}{2}+s}$ and $T \in \mathbb{R}_+$. We seek $\boldsymbol{v} \in \mathcal{C}^1\left([0,T];\mathbb{H}_J^{-\frac{1}{2}+s}\right) \cap \mathcal{C}\left([0,T];\mathbb{H}_J^{\frac{1}{2}+s}\right)$ and $\boldsymbol{g} \in \mathcal{C}^1\left([0,T];\mathbb{H}_J^{-\frac{1}{2}+s}\right)$ such that for all $t \in [0,T]$ it holds

$$c_m \partial_t \boldsymbol{v} = -\underline{\mathcal{J}}\boldsymbol{v} + \boldsymbol{i}_{\boldsymbol{\phi}_e}(t) - \boldsymbol{i}_{\text{ion}}(\boldsymbol{v},\boldsymbol{g}), \tag{4.29a}$$

$$\partial_t \boldsymbol{g} = \mathcal{HH}(\boldsymbol{v},\boldsymbol{g}), \tag{4.29b}$$

where $\boldsymbol{i}_{\boldsymbol{\phi}_e} \in \mathcal{C}\left([0,T];\mathbb{H}_J^{-\frac{1}{2}+s}\right)$ and initial conditions

$$\boldsymbol{v}(0) = \boldsymbol{v}_0 \quad \text{and} \quad \boldsymbol{g}(0) = \boldsymbol{g}_0. \tag{4.30}$$

As a consequence of Lemma 4.1 we have the following result:

Lemma 4.3. *For $s \geq 0$, the operator $\underline{\mathcal{J}} : \mathbb{H}_J^{\frac{1}{2}+s} \to \mathbb{H}_J^{-\frac{1}{2}+s}$ is continuous and coercive, i.e. there exists a compact operator $\underline{\mathsf{T}}_{\underline{\mathcal{J}}} : \mathbb{H}_J^{\frac{1}{2}+s} \to \mathbb{H}_J^{-\frac{1}{2}+s}$ such that*

$$\left\langle (\underline{\mathcal{J}} + \underline{\mathsf{T}}_{\underline{\mathcal{J}}})\boldsymbol{v}, \boldsymbol{v} \right\rangle_{\Gamma_0} \geq \mu \left\|\boldsymbol{v}\right\|^2_{\mathbb{H}^{\frac{1}{2}}}, \quad \textit{for all } \boldsymbol{v} \in \mathbb{H}_J^{\frac{1}{2}}, \tag{4.31}$$

and self–adjoint in the $\langle\cdot,\cdot\rangle_{\Gamma_0}$ duality product.

5. Existence and Uniqueness of Solutions for the Multiple Cell Problem

We now aim to prove existence and uniqueness of the multiple cells problem, Problem 4.2. We follow the approach presented for the single cell problem in [36], relying heavily on the use of analytic semigroup theory [33].

5.1. Analytic Semigroups.

We present the required concepts on analytic semigroups to study the well–posedness of Problem 4.2. We refer to [33, Chapter 2] for further details. Let X be a complex Banach space with norm $\|\cdot\|_X$ with dual X' and let $\mathcal{L}(X)$ be the space of linear endomorphisms on X.

Definition 5.1. [33, Definition 2.0.1] *Let $\mathsf{A} : D(\mathsf{A}) \subset X \to X$ be a linear operator with domain $D(\mathsf{A})$. Recall the* resolvent set $\rho(\mathsf{A}) := \{\lambda \in \mathbb{C} : \exists\ (\lambda\mathsf{I} - \mathsf{A})^{-1} \in \mathcal{L}(X)\}$ *and* resolvent operator $\mathsf{R}(\lambda,\mathsf{A}) := (\lambda I - \mathsf{A})^{-1}$ *for $\lambda \in \rho(\mathsf{A})$. The operator A is said to be* sectorial *if there are constants $\omega \in \mathbb{R}$, $\theta \in (\pi/2,\pi)$ and $M > 0$ such that*

(i) $S_{\theta,\omega} := \{\lambda \in \mathbb{C} :\ \lambda \neq \omega\ \wedge\ |\arg(\lambda-\omega)| < \theta\} \subset \rho(\mathsf{A})$,
(ii) $\|\mathsf{R}(\lambda,\mathsf{A})\|_{\mathcal{L}(X)} \leq \frac{M}{|\lambda-\omega|}$ *for all $\lambda \in S_{\theta,\omega}$.*

For $t > 0$, the properties stated in Definition 5.1 allow us to define a linear bounded operator $\exp(t\mathsf{A})$ in X by using the Dunford integral as follows

$$\exp(t\mathsf{A}) = \frac{1}{2\pi\imath}\int_{\omega+\gamma_{r,\eta}} \exp(t\lambda)\mathsf{R}(\lambda,\mathsf{A})d\lambda, \quad \forall\ t > 0, \tag{5.1}$$

where, for $r > 0$, $\eta \in (\pi/2,\theta)$, $\gamma_{r,\eta}$ is the curve $\{\lambda \in \mathbb{C} :\ |\arg\lambda| = \eta,\ |\lambda| \geq r\} \cup \{\lambda \in \mathbb{C} : |\arg\lambda| \leq \eta,\ |\lambda| = r\}$ oriented counterclockwise. Besides, we set

$$\exp(0\mathsf{A})x = x, \quad \forall\ x \in X. \tag{5.2}$$

Definition 5.2. [33, Definition 2.0.2] *Let $\mathsf{A} : D(\mathsf{A}) \subset X \to X$ be a sectorial operator. The family $\{\exp(t\mathsf{A}) :\ t > 0\}$ defined by (5.1) and (5.2) is said to be the* analytic semigroup generated by A in X.

The following proposition states sufficient conditions for an operator to be sectorial.

Proposition 5.3. [33, Proposition 2.1.11] *Let* $\mathsf{A} : D(\mathsf{A}) \subset X \to X$ *be a linear operator such that* $\rho(\mathsf{A})$ *contains a half plane* $\{\lambda \in \mathbb{C} : \ \mathfrak{Re}\lambda \geq \omega\}$*, and*

$$\|\lambda \mathsf{R}(\lambda, \mathsf{A})\|_{\mathcal{L}(X)} \leq M, \quad \mathfrak{Re}\ \lambda \geq \omega, \tag{5.3}$$

with $\omega \in \mathbb{R}$*,* $M > 0$*. Then the operator* A *is sectorial.*

Now let us now consider the following abstract evolution problem:

$$u'(t) = \mathsf{A}u(t) + f(t, u(t)), \quad t > 0, \quad u(0) = u_0 \tag{5.4}$$

where $\mathsf{A} : D(\mathsf{A}) \subset X \to X$ is a linear sectorial operator, f is a continuous function defined in $[0, T] \times X$ with values in X. One may define the different solution categories for the abstract evolution problem (5.4) as follows.

Definition 5.4. [33, Definitions 7.0.1 and 7.0.2] *We distinguish the following classes of solution for the abstract evolution problem* (5.4)*:*

(i) *A continuous function* $u : (0, T] \to X$ *such that* $u(t) \in X$ *for every* $t \in (0, T]$ *and* $f(\cdot, u(\cdot)) \in L^1([0, T]; X)$*, is said to be a* mild solution *of* (5.4) *in the interval* $[0, T]$ *if* u *satisfies*

$$u(t) = \exp(t\mathsf{A})u_0 + \int_0^t \exp\left[(t - s)\mathsf{A}\right] f(s, u(s))ds, \quad t \in [0, T]. \tag{5.5}$$

(ii) *A function* $u \in \mathcal{C}^1((0, T]; X) \cap \mathcal{C}((0, T]; D(\mathsf{A})) \cap \mathcal{C}([0, T]; X)$ *such that* $u(t) \in X$ *for all* $t \in [0, T]$ *is said to be a* classical solution *in the interval* $[0, T]$ *if* (5.4) *is satisfied for each* $t \in (0, T]$*.*

(iii) *A function* $u \in \mathcal{C}^1([0, T]; X) \cap \mathcal{C}([0, T]; D(\mathsf{A}))$ *such that* $u(t) \in X$ *for all* $t \in [0, T]$ *is said to be a* strict solution *in the interval* $[0, T]$ *if* (5.4) *is satisfied for each* $t \in [0, T]$*.*

Existence and uniqueness results together with conditions on the initial data u_0 and the non–linear function f have been established for mild, classical and strict solutions of (5.4) [33, Theorem 7.1.2 and Proposition 7.1.10].

5.2. **Existence and Uniqueness of the Multiple Cells Boundary Problem.** Using the previous definitions and results, we first prove that the operator $-\underline{\mathcal{J}}$, defined in (4.26), is actually sectorial, thus generating an analytic semigroup $\exp(-t\underline{\mathcal{J}})$ in $\mathbb{H}_J^{-\frac{1}{2}+s}$, for $s \geq \frac{1}{2}$.

Throughout this section, we work with complex valued Sobolev spaces, denoted also by $\mathbb{H}_J^s$, to fit in the framework for analytic semigroups presented previously. This impacts directly coercivity estimates in 4.3. For complex valued Sobolev spaces we should take the real part on the left hand side of the coercivity estimates. However, since the fundamental solution to the Laplace operator (3.1) is real valued, it holds

$$\mathfrak{Re}\left\{\left\langle \left(\underline{\mathcal{J}} + \underline{\mathsf{T}}_{\underline{\mathcal{J}}}\right)\boldsymbol{v}, \overline{\boldsymbol{v}}\right\rangle_{\Gamma_0}\right\} = \left\langle \left(\underline{\mathcal{J}} + \underline{\mathsf{T}}_{\underline{\mathcal{J}}}\right)\boldsymbol{v}, \overline{\boldsymbol{v}}\right\rangle_{\Gamma_0} \geq \mu \left\|\boldsymbol{v}\right\|^2_{\mathbb{H}_J^{\frac{1}{2}}}, \quad \text{for all } \boldsymbol{v} \in \mathbb{H}_J^{\frac{1}{2}}. \tag{5.6}$$

Proposition 5.5. *Let* $s \geq 0$ *and* $\boldsymbol{f} \in \mathbb{H}_J^{-\frac{1}{2}+s}$ *as in* (2.10)*. Then, there exists a unique* $\boldsymbol{v} \in \mathbb{H}_J^{\frac{1}{2}+s}$ *satisfying*

$$\left(\underline{\mathcal{J}} + \underline{\mathsf{T}}_{\underline{\mathcal{J}}}\right)\boldsymbol{v} = \boldsymbol{f}, \tag{5.7}$$

where $\underline{\mathsf{T}}_{\underline{\mathcal{J}}}$ *is the same as in Lemma 4.3.*

Proof. By the Lax–Milgram lemma and Lemma 4.3, the assertion holds for $s = 0$. The result for $s > 0$ follows from the regularity properties of boundary integral equations and mapping properties of the BIOs in smooth boundaries, [45, Theorem 3.2.2] and Theorem 3.3, respectively. □

Lemma 5.6. *For* $s \geq \frac{1}{2}$*, the operator* $\underline{\mathcal{J}} : \mathbb{H}_J^{\frac{1}{2}+s} \to \mathbb{H}_J^{-\frac{1}{2}+s}$ *generates an analytic semigroup* $\exp(-t\underline{\mathcal{J}})$ *on* $\mathbb{H}_J^{-\frac{1}{2}+s}$*.*

Proof. We take our cue from [40, Theorem 7.2.7]. Set $\underline{\mathcal{R}} := -(\underline{\mathcal{J}} + \underline{\mathsf{T}}_{\underline{\mathcal{J}}})$. According to Proposition 5.5, for $s = \frac{1}{2}$, the operator $\underline{\mathcal{R}}$ has the following mapping property $\underline{\mathcal{R}} : \mathbb{H}_J^1 \subset \mathbb{L}_J^2 \to \mathbb{L}_J^2$ with domain $D(\underline{\mathcal{R}}) = \mathbb{H}_J^1$. We define the set $S(\underline{\mathcal{R}})$ as

$$S(\underline{\mathcal{R}}) := \left\{\langle \underline{\mathcal{R}}\boldsymbol{u}, \overline{\boldsymbol{u}}\rangle_{\Gamma_0} : \ \boldsymbol{u} \in \mathbb{H}_J^1, \text{ such that } \|\boldsymbol{u}\|_{\mathbb{L}_J^2} = 1\right\}. \tag{5.8}$$

From Lemma 4.3 one can conclude that

$$S(\underline{\mathcal{R}}) \subset S := \{\lambda \in \mathbb{R} :\ \lambda < 0\} \subset \mathbb{C}. \tag{5.9}$$

Indeed we have for $\boldsymbol{u} \in \mathbb{H}^1_J$

$$-\langle \underline{\mathcal{R}}\boldsymbol{u}, \overline{\boldsymbol{u}}\rangle_{\Gamma_0} \geq \mu \left\|\boldsymbol{u}\right\|^2_{\mathbb{H}^{\frac{1}{2}}_J} \geq \mu \left\|\boldsymbol{u}\right\|^2_{\mathbb{L}^2_J}, \tag{5.10}$$

and therefore

$$\frac{\langle \underline{\mathcal{R}}\boldsymbol{u}, \overline{\boldsymbol{u}}\rangle_{\Gamma_0}}{\left\|\boldsymbol{u}\right\|^2_{\mathbb{L}^2_J}} \leq -\mu < 0. \tag{5.11}$$

On the other hand, it holds

$$\rho(\underline{\mathcal{R}}) \supset \Sigma := \{\lambda \in \mathbb{C} :\ \mathfrak{Re}\{\lambda\} \geq 0\} \tag{5.12}$$

Besides, we have that

$$\mathfrak{Re}\left\{\langle(\lambda \mathsf{I} - \underline{\mathcal{R}})\,\boldsymbol{v}, \overline{\boldsymbol{v}}\rangle_{\Gamma_0}\right\} = \mathfrak{Re}\left\{\left\langle\left(\lambda \mathsf{I} + \underline{\mathcal{J}} + \underline{\mathsf{T}}_{\underline{\mathcal{J}}}\right)\boldsymbol{v}, \overline{\boldsymbol{v}}\right\rangle_{\Gamma_0}\right\} \tag{5.13}$$

$$= \left\langle(\underline{\mathcal{J}} + \underline{\mathsf{T}}_{\underline{\mathcal{J}}})\boldsymbol{v}, \overline{\boldsymbol{v}}\right\rangle_{\Gamma_0} + \mathfrak{Re}\{\lambda\}\,\langle \boldsymbol{v}, \overline{\boldsymbol{v}}\rangle_{\Gamma_0} \tag{5.14}$$

$$\geq \mu \left\|\boldsymbol{v}\right\|^2_{\mathbb{H}^{\frac{1}{2}}_J} + \mathfrak{Re}\left\{\lambda\right\} \left\|\boldsymbol{v}\right\|^2_{\mathbb{L}^2_J} \tag{5.15}$$

$$\geq \mu \left\|\boldsymbol{v}\right\|^2_{\mathbb{H}^{\frac{1}{2}}_J} \tag{5.16}$$

holds for all $\boldsymbol{v} \in \mathbb{H}^{\frac{1}{2}}_J$ if $\lambda \in \Sigma$. In this case, the complex version of Lax–Milgram Lemma ensures that $\lambda \mathsf{I} - \underline{\mathcal{R}}$ has a bounded inverse for $\lambda \in \Sigma$. One may conclude that

$$d(\lambda, \overline{S}) = |\lambda|, \quad \text{for } \lambda \in \Sigma, \tag{5.17}$$

where $d(\lambda, \overline{S})$ is the distance between λ and the closure of the set S. Moreover, for $\lambda \in \Sigma$ and $\boldsymbol{u} \in \mathbb{H}^1_J$ such that $\left\|\boldsymbol{u}\right\|_{\mathbb{L}^2_J} = 1$, we have

$$d(\lambda, \overline{S}) \leq \left|\lambda - \langle \underline{\mathcal{R}}\boldsymbol{u}, \overline{\boldsymbol{u}}\rangle_{\Gamma_0}\right| \leq \left|\langle(\lambda \mathsf{I} - \underline{\mathcal{R}})\boldsymbol{u}, \overline{\boldsymbol{u}}\rangle_{\Gamma_0}\right| \leq \left\|(\lambda \mathsf{I} - \underline{\mathcal{R}})\boldsymbol{u}\right\|_{\mathbb{L}^2_J}. \tag{5.18}$$

Therefore, we have

$$\left\|\mathsf{R}(\lambda, -(\underline{\mathcal{J}} + \underline{\mathsf{T}}_{\mathcal{J}})\right\|_{\mathcal{L}\left(\mathbb{L}^2_J, \mathbb{L}^2_J\right)} = \left\|\mathsf{R}(\lambda, \underline{\mathcal{R}})\right\|_{\mathcal{L}\left(\mathbb{L}^2_J, \mathbb{L}^2_J\right)} \leq \frac{1}{|\lambda|}, \quad \lambda \in \Sigma. \tag{5.19}$$

By Proposition 5.3 we conclude that $\underline{\mathcal{R}}$ is a sectorial operator and generates an analytic semigroup of bounded linear operators in $\mathbb{L}^2_J$. Being $\mathbb{H}^1_J$ dense in $\mathbb{L}^2_J$ and $\underline{\mathsf{T}}_{\mathcal{J}} : \mathbb{H}^1_J \to \mathbb{L}^2_J$ a compact operator, from Proposition 2.4.3 in [33] we conclude that $-\underline{\mathcal{J}}$ itself is sectorial and also generates an analytic semigroup in $\mathbb{L}^2_J$. Finally, the mapping properties of the operator $\underline{\mathcal{J}}$ (*cf.* Lemma 4.3) guarantee the existence of an analytic semigroup in $\mathbb{H}^{-\frac{1}{2}+s}_J$, for $s \geq \frac{1}{2}$. □

We now recall the following result regarding the smoothness of the mappings $\mathcal{HH}(\boldsymbol{v}, \boldsymbol{g})$ and $\boldsymbol{i}_{\text{ion}}(\boldsymbol{v}, \boldsymbol{g})$.

Lemma 5.7. [36, Lemma 5.4] *Let $R > 0$ and $s > \frac{3}{2}$, then for all $\boldsymbol{v} \in \mathbb{H}^{-\frac{1}{2}+s}_J$ and $\boldsymbol{g} \in \mathbb{H}^{-\frac{1}{2}+s}_J$ such that $\left\|\boldsymbol{v}\right\|_{\mathbb{H}^{-\frac{1}{2}+s}_J} \leq R$ and $\left\|\boldsymbol{g}\right\|_{\mathbb{H}^{-\frac{1}{2}+s}_J} \leq R$, there exist constants C_0 depending on $\mathcal{HH}$ and $\boldsymbol{i}_{\text{ion}}$ and C_1 depending on R and the derivatives of $\mathcal{HH}$ and $\boldsymbol{i}_{\text{ion}}$ such that*

$$\left\|\mathcal{HH}(\boldsymbol{v}, \boldsymbol{g})\right\|_{\mathbb{H}^{-\frac{1}{2}+s}_J} + \left\|\boldsymbol{i}_{\text{ion}}(\boldsymbol{v}, \boldsymbol{g})\right\|_{\mathbb{H}^{-\frac{1}{2}+s}_J} \leq C_0 + C_1(R)\left(\left\|\boldsymbol{v}\right\|_{\mathbb{H}^{-\frac{1}{2}+s}_J} + \left\|\boldsymbol{g}\right\|_{\mathbb{H}^{-\frac{1}{2}+s}_J}\right). \tag{5.20}$$

Besides, for $\boldsymbol{v},\boldsymbol{v}',\boldsymbol{g},\boldsymbol{g}' \in \mathbb{H}_J^{-\frac{1}{2}+s}$ *such that* $\|\boldsymbol{v}\|_{\mathbb{H}_J^{-\frac{1}{2}+s}}, \|\boldsymbol{v}'\|_{\mathbb{H}_J^{-\frac{1}{2}+s}}, \|\boldsymbol{g}\|_{\mathbb{H}_J^{-\frac{1}{2}+s}}, \|\boldsymbol{g}'\|_{\mathbb{H}_J^{-\frac{1}{2}+s}} \leq R$*, there exists a constant* $C_2(R)$ *depending on* R *and the derivatives of* $\mathcal{HH}$ *and* $\boldsymbol{i}_{\text{ion}}$ *such that*

$$\|\mathcal{HH}(\boldsymbol{v},\boldsymbol{g}) - \mathcal{HH}(\boldsymbol{v}',\boldsymbol{g}')\|_{\mathbb{H}_J^{-\frac{1}{2}+s}} + \|\boldsymbol{i}_{\text{ion}}(\boldsymbol{v},\boldsymbol{g}) - \mathcal{HH}(\boldsymbol{v}',\boldsymbol{g}')\|_{\mathbb{H}_J^{-\frac{1}{2}+s}} \tag{5.21}$$

$$\leq C_2(R)\left(\|\boldsymbol{v}-\boldsymbol{v}'\|_{\mathbb{H}_J^{-\frac{1}{2}+s}} + \|\boldsymbol{g}-\boldsymbol{g}'\|_{\mathbb{H}_J^{-\frac{1}{2}+s}}\right). \tag{5.22}$$

We are now in position to enunciate the local existence and uniqueness results for 4.2.

Theorem 5.8 (Local Existence and Uniqueness of Problem 4.2)**.** *For* $s > \frac{3}{2}$*, let* $\boldsymbol{v}_0 \in \mathbb{H}_J^{-\frac{1}{2}+s}$ *and* $\boldsymbol{g}_0 \in \mathbb{H}_J^{-\frac{1}{2}+s}$ *be the initial conditions in Problem 4.2. Then, Problem 4.2 admits a unique mild solution* $\boldsymbol{v},\boldsymbol{g} \in \mathcal{C}([0,T],\mathbb{H}_J^{-\frac{1}{2}+s})$ *depending continuously on the initial data. Besides, Problem 4.2 also admits a unique classical solution which coincides with the mild solution. Finally, if* $\boldsymbol{v}_0 \in \mathbb{H}_J^{\frac{1}{2}+s}$ *then the solution is strict.*

Proof. For $s \geq \frac{1}{2}$, let us consider the augmented operator defined as

$$\mathcal{G} := \begin{pmatrix} \mathcal{J} \\ \mathbf{0} \end{pmatrix} : \mathbb{H}_J^{\frac{1}{2}+s} \times \mathbb{H}_J^{-\frac{1}{2}+s} \to \mathbb{H}_J^{-\frac{1}{2}+s} \times \mathbb{H}_J^{-\frac{1}{2}+s} \tag{5.23}$$

with domain $D(\mathcal{G}) = \mathbb{H}_J^{\frac{1}{2}+s} \times \mathbb{H}_J^{-\frac{1}{2}+s}$. Being $\underline{\mathcal{J}}$ sectorial, we have that $\mathcal{G}$ is sectorial as well, therefore generating an analytic semigroup in $\mathbb{H}_J^{-\frac{1}{2}+s} \times \mathbb{H}_J^{-\frac{1}{2}+s}$. The claim on mild, classical and strict solutions is a consequence of the analyticity of the semigroup generated by $\mathcal{G}$ [33, Chapter 7]. The condition $s > \frac{3}{2}$ comes from Lemma 5.7, which provides requirements in order to obtain the required smoothness of the nonlinearities $\mathcal{HH}(\boldsymbol{v},\boldsymbol{g})$ and $\boldsymbol{i}_{\text{ion}}(\boldsymbol{v},\boldsymbol{g})$ in the right Sobolev Spaces. □

Finally, for $\boldsymbol{u},\boldsymbol{v} \in \mathbb{H}_J^{\frac{1}{2}}$, we define the following bilinear form:

$$\mathsf{J}(\boldsymbol{u},\boldsymbol{v}) := \langle \underline{\mathcal{J}}\boldsymbol{u},\boldsymbol{v}\rangle_{\Gamma_0} : \mathbb{H}_J^{\frac{1}{2}} \times \mathbb{H}_J^{\frac{1}{2}} \mapsto \mathbb{R}. \tag{5.24}$$

6. Numerical Discretization

Though Problem 4.2 is valid in two and three dimensions, in what follows we present an efficient two-dimensional discretization scheme proved to be stable and convergent. Our numerical scheme is relies on two key elements. On one hand, we take advantage of smoothness inherent to biological cells by using Fourier polynomials for space discretization, which yields exponential convergence rates. On the other hand, we use a semi-implicit strategy in time to deal with the non–linearities arising in the terms $\boldsymbol{i}_{\text{ion}}(\boldsymbol{v},\boldsymbol{g})$ and $\mathcal{HH}(\boldsymbol{v},\boldsymbol{g})$.

6.1. Fourier Expansion.

We recall some useful results of Fourier analysis and refer to [30, Chapter 8] and [5, Section 6.5] for more details. Define the equivalence class of square integrable complex-valued functions as

$$L^2[0,2\pi] := \left\{\varphi : [0,2\pi] \to \mathbb{C} \text{ such that } \int_0^{2\pi} |f(\theta)|^2\, d\theta < \infty\right\}. \tag{6.1}$$

As usual, the $L^2[0,2\pi]$–norm is induced by the inner product:

$$(\varphi,\psi)_{L^2[0,2\pi]} = \int_0^{2\pi} \varphi(\theta)\overline{\psi(\theta)}d\theta. \tag{6.2}$$

The *Fourier series* of $\varphi \in L^2[0,2\pi]$ is

$$\varphi(\theta) = \sum_{k\in\mathbb{Z}} a_k \exp(\imath k\theta). \tag{6.3}$$

Let us define the *Fourier polynomials* $\varphi_k := \exp(\imath k\theta)$, for $k \in \mathbb{Z}$. Then, *Fourier coefficients* a_k in (6.3) are given by

$$a_k := \frac{1}{2\pi}(\varphi,\varphi_k)_{L^2[0,2\pi]} = \frac{1}{2\pi}\int_0^{2\pi} \varphi(\theta)\exp(-\imath k\theta)d\theta, \tag{6.4}$$

and Parseval's equality holds, i.e.

$$\|\varphi\|^2_{L^2[0,2\pi]} = 2\pi \sum_{k\in\mathbb{Z}} |a_k|^2 . \tag{6.5}$$

Definition 6.1 (Definition 8.1, [30]). *Let $0 \le p < \infty$. By $H^p[0,2\pi]$ we denote the space of all complex-valued functions $\varphi \in L^2[0,2\pi]$ with the property*

$$\sum_{k\in\mathbb{Z}} (1+k^2)^p |a_k|^2 < \infty, \tag{6.6}$$

for the Fourier coefficients a_k of φ. Notice that $H^0[0,2\pi]$ is equivalent to $L^2[0,2\pi]$.

Theorem 6.2 (Theorem 8.2, [30]). *The Sobolev space $H^p[0,2\pi]$ is a Hilbert space with the scalar product defined by*

$$(\varphi,\psi)_{H^p[0,2\pi]} = \sum_{k\in\mathbb{Z}} (1+k^2)^p a_k \overline{b_k}, \tag{6.7}$$

for $\varphi, \psi \in H^p[0,2\pi]$ with Fourier coefficients a_k and b_k, respectively. We can also define a semi–norm in $H^p[0,2\pi]$ as follows

$$|\varphi|^2_{H^p[0,2\pi]} = \sum_{k\in\mathbb{Z}} |k|^{2p} |a_k|^2 . \tag{6.8}$$

Finally, the set of Fourier polynomials is dense in $H^p[0,2\pi]$.

Set $\mathcal{S}_K := \operatorname{span}\{\varphi_k : \ k = -K, \dots, K\}$ as the finite dimensional space of Fourier polynomials up to degree K. We define the *partial Fourier summation* up to order K as follows

$$(\mathsf{P}_K\varphi)(\theta) := \sum_{|k|\le K} a_k \exp(\imath k\theta) \in \mathcal{S}_K. \tag{6.9}$$

Lemma 6.3. *Let $0 \le s \le p$. For $\varphi \in H^p[0,2\pi]$ there exists a constant $c(s,p)$ such that*

$$\|\varphi - \mathsf{P}_K\varphi\|_{H^s[0,2\pi]} \le c(s,p) K^{-(p-s)} |\varphi|_{H^p[0,2\pi]} . \tag{6.10}$$

Proof. Let $\varphi \in H^p[0,2\pi]$. Then

$$\|\varphi - \mathsf{P}_K\varphi\|^2_{H^s[0,2\pi]} = \sum_{|m|>K} (1+m^2)^s |a_m|^2 \tag{6.11}$$

$$\le \frac{1}{(1+K^2)^{p-s}} \sum_{|m|>K} (1+m^2)^p |a_m|^2 \tag{6.12}$$

$$\le 2^p K^{-2(p-s)} |\varphi|^2_{H^p[0,2\pi]} , \tag{6.13}$$

and the claim follows. □

Exponential convergence rates can be achieved when assuming analyticity as the next result shows [49] or [12, Sect. 5.1].

Lemma 6.4. *If φ is 2π-periodic analytic, with analyticity strip of width $2\eta_0$, i.e. for $|\mathrm{Im}(z)| \le \eta_0$, $\varphi(z)$ admits the absolutely convergent expansion*

$$\varphi(z) = \sum_{k\in\mathbb{Z}} \varphi_k \exp(\imath k z).$$

Then, for any η, $0 < \eta < \eta_0$, it holds

$$\|\varphi - \mathsf{P}_K\varphi\|_{H^s[0,2\pi]} \le a(s,\eta) K^s \exp(-\eta K), \tag{6.14}$$

with a and η independent of K.

Assume that Γ is the boundary of a simply connected bounded $\mathcal{C}^k$-domain, $k \in \mathbb{N}$ and that $\boldsymbol{\chi}(\theta)$ for $\theta \in [0, 2\pi)$ is a k–times regular and continuously differentiable 2π–periodic parametric representation of Γ. Then, for $0 \leq p \leq k$, we have the following characterization of the Sobolev space $H^p(\Gamma)$:

$$H^p(\Gamma) := \left\{ \varphi \in L^2(\Gamma) : \ \tau_{\boldsymbol{\chi}} \varphi \in H^p[0, 2\pi] \right\}, \tag{6.15}$$

where $\tau_{\boldsymbol{\chi}} : H^p(\Gamma) \to H^p[0, 2\pi]$ is defined as $\tau_{\boldsymbol{\chi}} \varphi := \varphi \circ \boldsymbol{\chi}$ for $\varphi \in H^p(\Gamma)$ and $p \geq 0$ and with inner product

$$(\varphi, \psi)_{H^p(\Gamma)} := (\tau_{\boldsymbol{\chi}} \varphi, \tau_{\boldsymbol{\chi}} \psi)_{H^p[0,2\pi]}. \tag{6.16}$$

for all $\varphi, \psi \in H^p(\Gamma)$. In particular, it holds

$$\|\varphi\|_{H^p(\Gamma)} = \|\tau_{\boldsymbol{\chi}} \varphi\|_{H^p[0,2\pi]}, \quad \forall\ \varphi \in H^p(\Gamma), \quad 0 \leq p \leq k. \tag{6.17}$$

Moreover, the definition of Sobolev spaces $H^p(\Gamma)$ is independent of the chosen parametric representation of the boundary Γ [30, Theorem 8.14].

6.2. **Semi-Implicit Time Stepping Scheme.** Define $\Upsilon_N := \{t_n\}_{n=0}^N$ as the uniform partition of the time interval $[0, T]$, for $T \in \mathbb{R}_+$ and $N \in \mathbb{N}$, where $t_n := n\tau$ and $\tau := T/N$ is the time step. Let

$$t_{n+\frac{1}{2}} := t_n + \frac{\tau}{2}, \qquad n = 0, \ldots, N-1, \tag{6.18}$$

be a midstep between t_n and t_{n+1}. For a time dependent quantity $\phi(t)$, we denote $\phi^n := \phi(t_n)$ and, for $n = 1, \ldots, N-1$, we consider the following quantities:

$$\bar{\partial}\phi^n := \frac{\phi^{n+1} - \phi^n}{\tau}, \qquad \phi^{n+\frac{1}{2}} := \phi\left(t_{n+\frac{1}{2}}\right), \tag{6.19}$$

$$\bar{\phi}^{n+\frac{1}{2}} := \frac{\phi^{n+1} + \phi^n}{2}, \qquad \widehat{\phi}^{n+\frac{1}{2}} := \frac{3\phi^n - \phi^{n-1}}{2}. \tag{6.20}$$

With these definitions one may derive the following time-local estimates:

Lemma 6.5. [24, Lemma 7] *Let $\varphi \in \mathcal{C}^2([0, T]; L^2[0, 2\pi])$, then it holds*

$$\left\| \bar{\varphi}^{n+\frac{1}{2}} - \varphi^{n+\frac{1}{2}} \right\|_{L^2[0,2\pi]} \leq \frac{1}{4}\tau^2 \max_{t \in [t_n, t_{n+1}]} \left\| \partial_t^2 \varphi(t) \right\|_{L^2[0,2\pi]}, \tag{6.21}$$

$$\left\| \hat{\varphi}^{n+\frac{1}{2}} - \varphi^{n+\frac{1}{2}} \right\|_{L^2[0,2\pi]} \leq \frac{5}{16}\tau^2 \max_{t \in [t_{n-1}, t_{n+1}]} \left\| \partial_t^2 \varphi(t) \right\|_{L^2[0,2\pi]}. \tag{6.22}$$

Furthermore, if $\varphi \in \mathcal{C}^3([0, T]; L^2[0, 2\pi])$,

$$\left\| \bar{\partial}\varphi^n - \partial_t \varphi^{n+\frac{1}{2}} \right\|_{L^2[0,2\pi]} \leq \frac{\tau^2}{48} \max_{t \in [t_n, t_{n+1}]} \left\| \partial_t^2 \varphi(t) \right\|_{L^2[0,2\pi]}. \tag{6.23}$$

6.3. **Fully Discrete Scheme.** In what follows, we assume that each subdomain boundary Γ_j, for $j = 1, \ldots, J$ admits a 2π–periodic $\mathcal{C}^\infty$-parametric representation denoted by $\boldsymbol{\chi}_j$. Given $K \in \mathbb{N}$, on each boundary we define the subspaces $\mathcal{S}_K(\Gamma_j) := \tau_{\boldsymbol{\chi}_j}^{-1} \circ \mathcal{S}_K$, for $j = 1, \ldots, J$ and

$$\mathbb{S}_{J,K} := \mathcal{S}_K(\Gamma_1) \times \cdots \times \mathcal{S}_K(\Gamma_J).$$

At each time step $t_n \in \Upsilon_N$, we seek sets of functions $\boldsymbol{v}_K^n$ and $\boldsymbol{g}_K^n \in \mathbb{S}_{J,K}$. Each one of them is an approximation at times t_n of the vector of continuous membrane potentials membrane potential $\boldsymbol{v}$ and gate variables $\boldsymbol{g}$, respectively.

With these elements, we state the semi-implicit time-space numerical discretization of Problem 4.2:

Problem 6.6 (Fully Discrete Boundary Integral Problem). Let $\boldsymbol{v}_K^0$, $\boldsymbol{v}_K^1$, $\boldsymbol{g}_K^0$ and $\boldsymbol{g}_K^1$, belonging to $\mathbb{S}_{J,K}$, be given. Then, for time steps $n = 1, \ldots, N-1$ we seek $\boldsymbol{v}_K^n$, $\boldsymbol{g}_K^n$ in $\mathbb{S}_{J,K}$ solutions of

$$\left\langle c_m \bar{\partial} \boldsymbol{v}_K^n, \boldsymbol{\varphi}_K \right\rangle_{\Gamma_0} + \mathsf{J}\left(\bar{\boldsymbol{v}}_K^{n+\frac{1}{2}}, \boldsymbol{\varphi}_K \right) = \left\langle \boldsymbol{i}_{\Phi_e}^{n+\frac{1}{2}}, \boldsymbol{\varphi}_K \right\rangle_{\Gamma_0} - \left\langle \boldsymbol{i}_{\text{ion}}\left(\hat{\boldsymbol{v}}_K^{n+\frac{1}{2}}, \hat{\boldsymbol{g}}_K^{n+\frac{1}{2}} \right), \boldsymbol{\varphi}_K \right\rangle_{\Gamma_0}, \tag{6.24a}$$

$$\left\langle \bar{\partial} \boldsymbol{g}_K^n, \boldsymbol{\varphi}_K \right\rangle_{\Gamma_0} = \left\langle \mathcal{H}\left(\hat{\boldsymbol{v}}_K^{n+\frac{1}{2}}, \hat{\boldsymbol{g}}_K^{n+\frac{1}{2}} \right), \boldsymbol{\varphi}_K \right\rangle_{\Gamma_0}, \tag{6.24b}$$

for all $\boldsymbol{\varphi}_K \in \mathbb{S}_{J,K}$, where the bilinear form J is defined in (5.24).

To properly solve Problem 6.6 values for $\boldsymbol{v}_K^0$, $\boldsymbol{v}_K^1$, $\boldsymbol{g}_K^0$ and $\boldsymbol{g}_K^1$ must be provided. A straightforward choice for $\boldsymbol{v}_K^0$ and $\boldsymbol{g}_K^0$ comes from initial conditions $\boldsymbol{v}_0$ and $\boldsymbol{g}_0$. For instance, one may choose $\boldsymbol{v}_K^0 := \underline{\hat{\mathsf{P}}}_K \boldsymbol{v}_0$ and $\boldsymbol{g}_K^0 := \underline{\hat{\mathsf{P}}}_K \boldsymbol{g}^0$, where $\underline{\hat{\mathsf{P}}}_K : \mathbb{H}_J^p \to \mathbb{S}_{J,K}$ is defined as $\underline{\hat{\mathsf{P}}}_K := (\hat{\mathsf{P}}_{K,1}, \cdots, \hat{\mathsf{P}}_{K,J})$ and $\hat{\mathsf{P}}_{K,j} := \tau_{\boldsymbol{\chi}_j}^{-1} \circ \mathsf{P}_K \circ \tau_{\boldsymbol{\chi}_j}$, for $j = 1, \ldots, J$ and $p \geq 0$.

Values for $\boldsymbol{v}_K^1$ and $\boldsymbol{g}_K^1$ are estimated by solving the following *predictor–corrector algorithm* summarized in Algorithm 6.7 (*cf.* [51, Chapter 13] and [22]), as it has been done in [24] for the single biological cell case:

Algorithm 6.7 (Predictor–Corrector method). Set $\boldsymbol{w}_h^0 := \boldsymbol{v}_h^0$ and $\boldsymbol{r}_h^0 := \boldsymbol{g}_h^0$, then we proceed as follows:

(I) *Predictor.* We first construct predictions $\boldsymbol{w}_h^1$ and $\boldsymbol{r}_h^1$, for $\boldsymbol{v}_h^1$ and $\boldsymbol{g}_h^1$, respectively, by solving the linear system:

$$\begin{aligned} \left\langle c_m \bar{\partial} \boldsymbol{w}_K^0, \boldsymbol{\varphi}_K \right\rangle_{\Gamma_0} + \mathsf{J}\left(\bar{\boldsymbol{w}}_K^{\frac{1}{2}}, \boldsymbol{\varphi}_K\right) &= \left\langle \boldsymbol{i}_{\Phi_e}^{\frac{1}{2}}, \boldsymbol{\varphi}_K \right\rangle_{\Gamma_0} - \left\langle \boldsymbol{i}_{\text{ion}}\left(\boldsymbol{v}_K^0, \boldsymbol{g}_K^0\right), \boldsymbol{\varphi}_K \right\rangle_{\Gamma_0}, \\ \left\langle \bar{\partial} \boldsymbol{r}_K^0, \boldsymbol{\varphi}_K \right\rangle_{\Gamma_0} &= \left\langle \mathcal{HH}\left(\boldsymbol{w}_K^0, \boldsymbol{r}_K^0\right), \boldsymbol{\varphi}_K \right\rangle_{\Gamma_0}, \end{aligned}$$

for all $\boldsymbol{\varphi}_K \in \mathbb{S}_{J,K}$. Notice that both $\boldsymbol{w}_h^1$ and $\boldsymbol{r}_h^1$ appear through the definitions given in Subsection 6.2.

(II) *Corrector.* We now correct $\boldsymbol{w}_K^1$ and $\boldsymbol{r}_K^1$, to obtain final values for $\boldsymbol{v}_K^1$ and $\boldsymbol{g}_K^1$ through

$$\begin{aligned} \left\langle c_m \bar{\partial} \boldsymbol{v}_K^0, \boldsymbol{\varphi}_K \right\rangle_{\Gamma_0} + \mathsf{J}\left(\bar{\boldsymbol{v}}_h^{\frac{1}{2}}, \boldsymbol{\varphi}_K\right) &= \left\langle \boldsymbol{i}_{\Phi_e}^{\frac{1}{2}}, \boldsymbol{\varphi}_K \right\rangle - \left\langle \boldsymbol{i}_{\text{ion}}\left(\bar{\boldsymbol{w}}_K^{\frac{1}{2}}, \bar{\boldsymbol{r}}_K^{\frac{1}{2}}\right), \boldsymbol{\varphi}_K \right\rangle_{\Gamma_0}, \\ \left\langle \bar{\partial} \boldsymbol{g}_K^0, \boldsymbol{\varphi}_k \right\rangle_{\Gamma_0} &= \left\langle \mathcal{HH}\left(\bar{\boldsymbol{w}}_K^{\frac{1}{2}}, \bar{\boldsymbol{r}}_K^{\frac{1}{2}}\right), \boldsymbol{\varphi}_K \right\rangle, \end{aligned}$$

for all $\boldsymbol{\varphi}_K \in \mathbb{S}_{J,K}$. Again, both $\boldsymbol{v}_K^1$ and $\boldsymbol{g}_K^1$ are implicit in the previous equations through the quantities defined in Subsection 6.2.

6.4. **Convergence Analysis.** We seek to prove bounds for the total approximation error for the transmembrane potential and gate variables. In particular, we are interested in measuring the errors $\boldsymbol{v}(t_n) - \boldsymbol{v}^n$ and $\boldsymbol{g}(t_n) - \boldsymbol{g}^n$ in the $\mathbb{L}_J^2$–norm for all $t_n \in \Upsilon_N$.

For $\boldsymbol{v} \in \mathcal{C}^1([0,T], \mathbb{H}_J^{\frac{1}{2}})$ and $\lambda \in \mathbb{R}_+$, let us define $\boldsymbol{v}_\lambda := \exp(-\lambda t)\boldsymbol{v}$, for $t \in [0,T]$. Then

$$\partial_t \boldsymbol{v} = \lambda \exp(\lambda t)\boldsymbol{v}_\lambda + \exp(\lambda t)\partial_t \boldsymbol{v}_\lambda. \tag{6.25}$$

Consequently, one can rewrite Problem 4.2 in terms $\boldsymbol{v}_\lambda$ as presented in Problem 6.8.

Problem 6.8. Let $s > \frac{3}{2}$ and $\lambda > 0$, $\boldsymbol{v}_0 \in \mathbb{H}_J^{\frac{1}{2}+s}$, $\boldsymbol{g}_0 \in \mathbb{H}_J^{-\frac{1}{2}+s}$ and $T \in \mathbb{R}_+$. We seek $\boldsymbol{v} \in \mathcal{C}^1([0,T], \mathbb{H}_J^{-\frac{1}{2}+s}) \cap \mathcal{C}([0,T], \mathbb{H}_J^{\frac{1}{2}+s})$ and $\boldsymbol{g} \in \mathcal{C}^1([0,T], \mathbb{H}_J^{-\frac{1}{2}+s})$ such that for all $t \in [0,T]$ it holds

$$c_m \partial_t \boldsymbol{v}_\lambda = -\underline{\mathcal{J}}_\lambda \boldsymbol{v}_\lambda + \exp(-\lambda t)\left(\boldsymbol{i}(t) - \boldsymbol{i}_{\text{ion}}\left(\exp(\lambda t)\boldsymbol{v}_\lambda, \boldsymbol{g}\right)\right), \tag{6.26a}$$

$$\partial_t \boldsymbol{g} = \mathcal{HH}\left(\exp(\lambda t)\boldsymbol{v}_\lambda, \boldsymbol{g}\right), \tag{6.26b}$$

where $\boldsymbol{i}_{\boldsymbol{\phi}_e} \in \mathcal{C}\left([0,T]; \mathbb{H}_J^{-\frac{1}{2}+s}\right)$ and $\underline{\mathcal{J}}_\lambda := c_m \lambda\, \mathsf{I} + \underline{\mathcal{J}}$.

Remark 6.9. We can choose λ large so that $\underline{\mathcal{J}}_\lambda$ becomes elliptic. In fact, it is enough to pick

$$\lambda \geq \lambda_{\min} := \frac{\left\| \underline{\mathsf{T}}_{\underline{\mathcal{J}}} \right\|_{\mathcal{L}\left(\mathbb{H}_J^{\frac{1}{2}}, \mathbb{L}_J^2\right)}}{c_m}. \tag{6.27}$$

Indeed, we have

$$\begin{aligned} \left\langle \underline{\mathcal{J}}_\lambda \boldsymbol{v}, \boldsymbol{v} \right\rangle_{\Gamma_0} &= \left\langle (\underline{\mathcal{J}} + c_m \lambda\, \mathsf{I} + \underline{\mathsf{T}}_{\underline{\mathcal{J}}} - \underline{\mathsf{T}}_{\underline{\mathcal{J}}})\boldsymbol{v}, \boldsymbol{v} \right\rangle_{\Gamma_0} \\ &\geq \mu \left\| \boldsymbol{v} \right\|_{\mathbb{H}_J^{\frac{1}{2}}}^2 + \underbrace{\left(c_m \lambda - \left\| \underline{\mathsf{T}}_{\underline{\mathcal{J}}} \right\|_{\mathcal{L}\left(\mathbb{H}_J^{\frac{1}{2}}, \mathbb{L}_J^2\right)} \right)}_{\geq 0} \left\| \boldsymbol{v} \right\|_{\mathbb{L}_J^2}^2 \geq \mu \left\| \boldsymbol{v} \right\|_{\mathbb{H}_J^{\frac{1}{2}}}^2, \end{aligned} \tag{6.28}$$

with μ coming from (5.6), and where the mapping boundedness of the map $\underline{\mathsf{T}}_{\underline{\mathcal{J}}} : \mathbb{H}_J^{\frac{1}{2}} \to \mathbb{L}_J^2$ is a consequence of the smoothing properties of the BIOs (*cf.* [48, Section 6.1] and [45, Theorem 3.5.5]).

The use of the $\mathbb{H}^{\frac{1}{2}}_J$–ellipticity of $\underline{\mathcal{J}}_\lambda$, for λ large enough, requires first to compute the error in the $\mathbb{L}^2_J$–norm of $\boldsymbol{v}_\lambda(t_n) - \boldsymbol{v}^n_\lambda$ and $\boldsymbol{g}_\lambda(t_n) - \boldsymbol{g}^n_\lambda$ for $t_n \in \Upsilon_N$. Indeed, it holds

$$\|\boldsymbol{v}(t_n) - \boldsymbol{v}^n\|_{\mathbb{L}^2_J} = \exp(\lambda t_n)\, \|\boldsymbol{v}_\lambda(t_n) - \boldsymbol{v}^n_\lambda\|_{\mathbb{L}^2_J}\,, \quad \text{and} \tag{6.29a}$$

$$\|\boldsymbol{g}(t_n) - \boldsymbol{g}^n\|_{\mathbb{L}^2_J} = \exp(\lambda t_n)\, \|\boldsymbol{g}_\lambda(t_n) - \boldsymbol{g}^n_\lambda\|_{\mathbb{L}^2_J}\,. \tag{6.29b}$$

We drop momentarily the explicit time-dependence in n, reintroducing the corresponding superscript in Section 6.5. The forthcoming error analysis relies on the one presented in [24, Section 6] and hinges on the so–called *elliptic projection* $\boldsymbol{w}_\lambda$, defined as the solution of the following variational problem:

$$\mathsf{J}_\lambda(\boldsymbol{v}_\lambda - \boldsymbol{w}_\lambda, \boldsymbol{\varphi}) = 0, \quad \text{for all } \boldsymbol{\varphi} \in \mathbb{H}^{\frac{1}{2}}_J. \tag{6.30}$$

One may similarly define the *discrete elliptic projection* $\boldsymbol{w}_{\lambda,K}$, unique solution of

$$\mathsf{J}_\lambda(\boldsymbol{v}_\lambda - \boldsymbol{w}_{\lambda,K}, \boldsymbol{\varphi}_K) = 0, \quad \text{for all } \boldsymbol{\varphi}_K \in \mathbb{S}_{J,K}. \tag{6.31}$$

In particular, we notice that if $\boldsymbol{v}_\lambda \in \mathbb{S}_{J,K}$, then $\boldsymbol{v}_\lambda \equiv \boldsymbol{w}_{\lambda,K}$. We decompose the error between the exact solution $\boldsymbol{v}_\lambda$ and the discrete approximation $\boldsymbol{v}_{\lambda,K} \in \mathbb{S}_{J,K}$ as

$$\boldsymbol{v}_\lambda - \boldsymbol{v}_{\lambda,K} = \boldsymbol{v}_\lambda - \boldsymbol{w}_{\lambda,K} + \boldsymbol{w}_{\lambda,K} - \boldsymbol{v}_{\lambda,K} \tag{6.32}$$

and study each contribution independently.

6.4.1. *Properties of the Elliptic Projector* J_λ. Let us consider the following auxiliary problem:

Problem 6.10. For a given $\boldsymbol{f} \in \mathbb{H}^{-\frac{1}{2}}_J$, find $\boldsymbol{w}_\lambda \in \mathbb{H}^{\frac{1}{2}}_J$ such that

$$\mathsf{J}_\lambda(\boldsymbol{w}_\lambda, \boldsymbol{\varphi}) = \langle \boldsymbol{f}, \boldsymbol{\varphi} \rangle_{\Gamma_0}\,, \quad \text{for all } \boldsymbol{\varphi} \in \mathbb{H}^{\frac{1}{2}}_J. \tag{6.33}$$

For a parameter $\lambda \in \mathbb{R}_+$ large as in Remark 6.9, continuity and ellipticity of J_λ is ensured by Lemma 4.3 together with Remark 6.9. Consequently, the Lax–Milgram lemma [48, Theorem 3.4] guarantees existence and uniqueness for Problem 6.10. It also holds

$$\|\boldsymbol{w}_\lambda\|_{\mathbb{H}^{\frac{1}{2}}_J} \leq \frac{1}{\mu}\, \|\boldsymbol{f}\|_{\mathbb{H}^{-\frac{1}{2}}_J}\,, \tag{6.34}$$

where μ is the ellipticiy constant of J_λ in (6.28). Cea's Lemma [48, Theorem 8.1] allows us to extend those properties to the discrete setting in $\mathbb{S}_{J,K}$. It provides as well the best approximation error estimate:

$$\|\boldsymbol{w}_\lambda - \boldsymbol{w}_{\lambda,K}\|_{\mathbb{H}^{\frac{1}{2}}_J} \leq \frac{\alpha_\lambda}{\mu} \inf_{\boldsymbol{\varphi}_K \in \mathbb{S}_{J,K}} \|\boldsymbol{w}_\lambda - \boldsymbol{\varphi}_K\|_{\mathbb{H}^{\frac{1}{2}}_J}\,, \tag{6.35}$$

where $\alpha_\lambda := c_m \lambda + \|\underline{\mathcal{J}}\|_{\mathcal{L}\left(\mathbb{H}^{\frac{1}{2}}_J, \mathbb{H}^{-\frac{1}{2}}_J\right)}$ is the continuity constant of J_λ.

Lemma 6.11. *Assume* $\boldsymbol{f} \in \mathbb{H}^{-\frac{1}{2}+s}_J$ *and boundaries* Γ_j *to be of class* $\mathcal{C}^\infty$*, for* $j = 1, \ldots, J$*. Then, for* $s > 0$*, the solution* $\boldsymbol{w}_\lambda$ *of Problem 6.10 belong to* $\mathbb{H}^{-\frac{1}{2}+s}_J$ *and the following* a priori *estimate is valid*

$$\|\boldsymbol{w}_\lambda\|_{\mathbb{H}^{\frac{1}{2}+s}_J} \leq c(s) \left(\|\boldsymbol{w}_\lambda\|_{\mathbb{H}^{\frac{1}{2}}_J} + \|\boldsymbol{f}\|_{\mathbb{H}^{-\frac{1}{2}+s}_J} \right), \tag{6.36}$$

where $c(s)$ *is a positive constant depending on* s*.*

Proof. Follows directly from BIOs regularity properties for smooth domains (*cf.* [45, Theorem 3.2.2]). □

6.4.2. *Elliptic Projection – Error Estimates.* The triangle inequality yields

$$\|\boldsymbol{v}_\lambda - \boldsymbol{w}_{\lambda,K}\|_{\mathbb{H}^{\frac{1}{2}}_J} \leq \|\boldsymbol{v}_\lambda - \boldsymbol{w}_\lambda\|_{\mathbb{H}^{\frac{1}{2}}_J} + \|\boldsymbol{w}_\lambda - \boldsymbol{w}_{\lambda,K}\|_{\mathbb{H}^{\frac{1}{2}}_J}\,. \tag{6.37}$$

However, from the definition of elliptic projection, namely equation (6.30), and the ellipticity of the bilinear form $\mathsf{J}_\lambda(\cdot,\cdot)$ we have $\|\boldsymbol{v}_\lambda - \boldsymbol{w}_\lambda\|_{\mathbb{H}^{\frac{1}{2}}_J} = 0$. Therefore, it holds

$$\|\boldsymbol{v}_\lambda - \boldsymbol{w}_{\lambda,K}\|_{\mathbb{H}^{\frac{1}{2}}_J} \leq \|\boldsymbol{w}_\lambda - \boldsymbol{w}_{\lambda,K}\|_{\mathbb{H}^{\frac{1}{2}}_J}\,. \tag{6.38}$$

Using estimates (6.38) and (6.35) we obtain

$$\|\boldsymbol{v}_\lambda - \boldsymbol{w}_{\lambda,K}\|_{\mathbb{H}_J^{\frac{1}{2}}} \leq \|\boldsymbol{w}_\lambda - \boldsymbol{w}_{\lambda,K}\|_{\mathbb{H}_J^{\frac{1}{2}}} \leq \frac{\alpha_\lambda}{\mu} \inf_{\boldsymbol{\varphi}_K \in \mathbb{S}_{J,K}} \|\boldsymbol{w}_\lambda - \boldsymbol{\varphi}_K\|_{\mathbb{H}_J^{\frac{1}{2}}}, \tag{6.39}$$

Recall $\boldsymbol{\chi}_j$ is the 2π–periodic parametric representation of the boundary Γ_j, for $j = 1, \ldots, J$. Expanding the total error bound (6.39) into its components over each boundary Γ_j and recalling (6.17) we have

$$\|\boldsymbol{v}_\lambda - \boldsymbol{w}_{\lambda,K}\|_{\mathbb{H}_J^{\frac{1}{2}}} \leq \frac{\alpha_\lambda}{\mu} \sum_{j=1}^{J} \inf_{\varphi_{j,K} \in \mathcal{S}_K(\Gamma_j)} \left\| \tau_{\boldsymbol{\chi}_j} w_j^\lambda - \tau_{\boldsymbol{\chi}_j} \varphi_{j,K} \right\|_{H^{\frac{1}{2}}[0,2\pi]}, \tag{6.40}$$

where $\boldsymbol{w}_\lambda = (w_1^\lambda, \ldots, w_J^\lambda)$ with elements $w_j^\lambda \in H^{\frac{1}{2}}[0, 2\pi]$, $\boldsymbol{w}_{\lambda,K} = (w_{1,K}^\lambda, \ldots, w_{J,K}^\lambda)$ and $\boldsymbol{\varphi}_K = (\varphi_{1,K}, \ldots, \varphi_{J,K})$ are such that $w_{j,K}^\lambda$, $\varphi_{j,K} \in \mathcal{S}_K(\Gamma_j)$, for $j = 1, \ldots, J$. By Lemma 6.11, we can employ the Aubin-Nitsche trick [45, Sect. 4.2.5] to shift the error norm from $\mathbb{H}_J^{\frac{1}{2}}$ to $\mathbb{L}_J^2$. Then, by Lemma6.3, we obtain the following error estimate

$$\|\boldsymbol{v}_\lambda - \boldsymbol{w}_{\lambda,K}\|_{\mathbb{L}_J^2} \leq \frac{\alpha_\lambda}{\mu} c(p) J K^{-p} \left| v_j^\lambda \right|_{H^p[0,2\pi]}, \tag{6.41}$$

by acknowledging that $\boldsymbol{v}_\lambda = \boldsymbol{w}_\lambda$. Furthermore, if the solution is 2π-periodic analytic, we can use Lemma 6.4 to derive the following bound

$$\|\boldsymbol{v}_\lambda - \boldsymbol{w}_{\lambda,K}\|_{\mathbb{L}_J^2} \leq \frac{\alpha_\lambda}{\mu} J\Theta \exp(-\eta K), \tag{6.42}$$

where Θ and η are positive constants independent of K and the number of cells J. Finally, using (6.29a), (6.29b) to retrieve $\boldsymbol{v}_\lambda$ from $\boldsymbol{v}$, we can state the following theorem:

Theorem 6.12. *Let $\boldsymbol{v}$ be the solution of Problem 4.2 and assume that it satisfies the analyticity conditions of Lemma 6.4. Then, for all times $t \in [0, T]$, the following error estimate holds*

$$\|\boldsymbol{v} - \boldsymbol{w}_K\|_{\mathbb{L}_J^2} \leq \frac{\alpha_\lambda}{\mu} J\Theta \exp(\lambda T) \exp(-\eta K), \tag{6.43}$$

where Θ and η are positive constants independent of K and the number of cells J.

6.5. **Convergence estimates.** We now return our attention to the time discretization. At a time $t_n \in \Upsilon_N$, we split the full error $\boldsymbol{v}^n - \boldsymbol{v}_K^n$ as follows

$$\boldsymbol{v}^n - \boldsymbol{v}_K^n = \underbrace{(\boldsymbol{v}^n - \boldsymbol{w}_K^n)}_{=:\boldsymbol{\rho}^n} + \underbrace{(\boldsymbol{w}_K^n - \boldsymbol{v}_K^n)}_{=:\boldsymbol{\theta}^n}, \tag{6.44}$$

where $\boldsymbol{w}_K^n$ is defined as in (6.31) for each time step t_n, $n = 0, \ldots, N$. Due to Lemma 6.4, one concludes that $\boldsymbol{\rho}^n$ is bounded in the $\mathbb{L}_J^2$–norm by Theorem 6.12. Following the error analysis presented [24, Section 6.3], one can derive the next result for $\boldsymbol{\theta}^n$, for $n = 0, \ldots, N$.

Lemma 6.13. *Let $\boldsymbol{v}$ and $\boldsymbol{g}$ be the solution of Problem 4.2 for initial data $\boldsymbol{v}_0$ and $\boldsymbol{g}_0$. Besides, let $\boldsymbol{v}_K^n$ and $\boldsymbol{g}_K^n$ be the solution of Problem 6.6 for initial boundary data $\boldsymbol{v}_K^0$, $\boldsymbol{v}_K^1$, $\boldsymbol{g}_K^0$ and $\boldsymbol{g}_K^1$ in $\mathbb{S}_{J,K}$, for $n = 1, \ldots, N-1$. Then, it holds:*

$$\left\|\boldsymbol{\theta}^{n+1}\right\|_{\mathbb{L}_J^2}^2 \leq c_1 \left(\left\|\boldsymbol{\theta}^1\right\|_{\mathbb{L}_J^2}^2 + \tau \left\|\boldsymbol{\theta}^0\right\|_{\mathbb{L}_J^2}^2 + \tau \sum_{j=1}^{n} (1 + \delta_1 \tau)^{-(j+1)} \left\| \hat{\boldsymbol{g}}_K^{j+\frac{1}{2}} - \underline{\hat{\mathsf{P}}}_K \boldsymbol{g}^{j+\frac{1}{2}} \right\|_{\mathbb{L}_J^2}^2 + \left(\exp(-\eta K) + \tau^2\right)^2 \right),$$

and

$$\begin{aligned} \left\|\boldsymbol{g}^{n+1} - \boldsymbol{g}_K^{n+1}\right\|_{\mathbb{L}_J^2} \leq c_2 \Big(& \left\|\boldsymbol{g}^1 - \boldsymbol{g}_K^1\right\|_{\mathbb{L}_J^2} + \tau \left\|\boldsymbol{g}^0 - \boldsymbol{g}_K^0\right\|_{\mathbb{L}_J^2} \\ & + \tau \sum_{j=1}^{n} (1 + \delta_2 \tau)^{-(j+1)} \left\| \hat{\boldsymbol{v}}_K^{j+\frac{1}{2}} - \underline{\hat{\mathsf{P}}}_K \boldsymbol{v}^{j+\frac{1}{2}} \right\|_{\mathbb{L}_J^2} + \tau^2 \Big) \end{aligned}$$

where c_1, c_2, δ_1 and δ_2 are positive constants independent of τ and K and depending on the constants α_λ, μ, J and Θ from Theorem 6.12.

With this last result, we can now state the main convergence result of our numerical scheme:

Parameters	Symbol	Value	Units
Extracellular conductivity	σ_e	20	mS/cm
Intracellular conductivity	σ_i	5	mS/cm
Membrane capacitance	c_m	1	μF/cm^2
Cell radius	R	7.5×10^{-4}	cm

TABLE 1. Simulation parameters

Theorem 6.14. *Under the same hypotheses of Lemma 6.13, if $\boldsymbol{v}_K^1$ and $\boldsymbol{g}_K^1$ are chosen according to Algorithm 6.7, the following error estimates hold*

$$\|\boldsymbol{v}^n - \boldsymbol{v}_K^n\|_{\mathbb{L}_J^2} \leq c_C \left(\left\|\boldsymbol{v}_K^0 - \boldsymbol{v}_0\right\|_{\mathbb{L}_J^2} + \left\|\boldsymbol{g}_0 - \boldsymbol{g}_K^0\right\|_{\mathbb{L}_J^2} + \exp(-\eta K) + \tau^2 \right),$$

and

$$\|\boldsymbol{g}^n - \boldsymbol{g}_K^n\|_{\mathbb{L}_J^2} \leq c_C \left(\left\|\boldsymbol{v}_K^0 - \boldsymbol{v}_0\right\|_{\mathbb{L}_J^2} + \left\|\boldsymbol{g}_0 - \boldsymbol{g}_K^0\right\|_{\mathbb{L}_J^2} + \exp(-\eta K) + \tau^2 \right),$$

for $n = 2, \ldots, N$, with c_C and δ are positive constants independent of τ and K and depending on the constants α_λ, μ, J and Θ from Theorem 6.12.

Proof. The proof is a direct consequence of Lemma 6.13, Theorem 6.12 and approximation properties of $\boldsymbol{v}_K^1$ and $\boldsymbol{g}_K^1$ given in Algorithm 6.7. For details, we refer to [51, Theorem 13.5]. and [24, Theorem 4]. □

6.6. **Stability Analysis.** We now provide stability conditions for the numerical scheme given in Problem 6.6. As shown in [24, Section 5], two time-dependent systems are coupled: one describing the evolution of HH gate variables (6.24b), while the second model depicts the transmembrane voltage and current (6.24a). We establish bounds for the time-spacing τ in both cases and define a global criterion to be later used in numerical simulations.

In the HH model, the system of gating variables (6.24b) can be arranged as follows [17]:

$$\partial_t g_j = -\frac{g_j - g_j^\infty(v_j)}{\tau_j(v_j)}, \qquad g_j(0) = g_{j,0},$$

where g_j represents the gate variable related to the cellular membrane Γ_j, $j = 1, \ldots, J$, with

$$g_j^\infty(v_j) = \frac{\alpha_j(v_j)}{\alpha_j(v_j) + \beta_j(v_j)} \quad \text{and} \quad \tau_j(v_j) = \frac{1}{\alpha_j(v_j) + \beta_j(v_j)},$$

for a given transmembrane potential v_j. Moreover, assume that the ionic current $i_{\text{ion},j}$ can be written as the product of a function depending solely on g_j and v_j, i.e.

$$i_{\text{ion},j}(v_j, g_j) = \mathcal{H}_j(g_j)\, v_j. \tag{6.45}$$

Based on this assumption, we can state the following result regarding the stability of Problem 6.6 (*cf.* [24, Theorem 3]).

Theorem 6.15. *Let $\boldsymbol{v}_K^n$, $\boldsymbol{g}_K^n$ for $n = 2, \ldots, N-1$, denote solutions of the fully discrete Problem 6.6 at times $t_n \in \Upsilon_N$. If $v_{\max} > 0$ denotes the bounded maximum value for the transmembrane potential for all biological cells, the numerical scheme proposed is stable for all positive time-spacings τ such that*

$$\tau < \min\left\{ \frac{c_m}{\mathcal{H}_{1,\max}}, \cdots, \frac{c_m}{\mathcal{H}_{J,\max}}, \frac{2}{3} \min_{|v_1| \leq v_{\max}} \frac{1}{\alpha_1(v_1) + \beta_1(v_1)}, \ldots, \frac{2}{3} \min_{|v_J| \leq v_{\max}} \frac{1}{\alpha_J(v_J) + \beta_J(v_J)} \right\}$$

where α_j, β_j, $m = 1, \ldots, J$ denote the v_j-dependent gate model variables and $\mathcal{H}_{j,\max}$ is the maximum value for $\mathcal{H}_j$.

7. Numerical Results

The numerical scheme presented in Section 6 was implemented in C++ with basic linear algebra routines coming from Lapack [3]. Simulations where run on a AMD FX-8350 Eight-Core processor at 2.8 GHz. In all the simulations the biological cells are assumed to be circles of equal radius. Table 1 contains a list of parameters employed in the computations presented here.

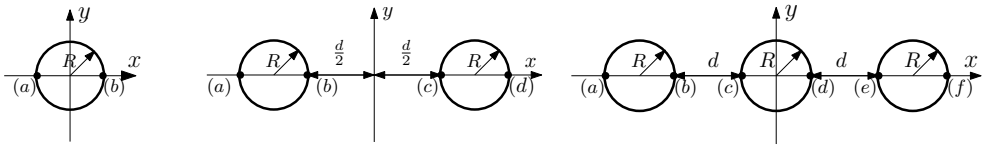

FIGURE 1. Configurations used in the convergence analysis. We consider the three following settings wherein all cells are of radius R. The distance d between cells will be specified later. Figure (i) portrays a single cell centered at the origin of the coordinate system; Figure (ii) portrays two cells separated by a distance d to be specified later; and, Figure (ii) portrays three cells separated by a distance d to be specified later. In the three scenarios we assume that the electric field $\mathbf{E}$ is as in (7.1) constant in space and time.

K	τ	Error Single Cell	Error Two Cells	Error Three Cells
1	1.64×10^{-3}	7.36×10^{-1}	4.98×10^{-1}	3.77×10^{-1}
2	1.00×10^{-3}	2.98×10^{-2}	9.27×10^{-2}	2.45×10^{-1}
3	6.06×10^{-4}	4.37×10^{-2}	5.06×10^{-2}	1.02×10^{-1}
4	3.67×10^{-4}	5.84×10^{-4}	2.74×10^{-2}	6.82×10^{-2}
5	2.23×10^{-4}	2.23×10^{-5}	1.55×10^{-2}	3.82×10^{-2}
6	1.35×10^{-4}	1.25×10^{-5}	8.99×10^{-3}	2.49×10^{-2}
7	8.20×10^{-5}	3.03×10^{-6}	5.26×10^{-3}	1.55×10^{-2}
8	4.97×10^{-5}	2.80×10^{-7}	3.10×10^{-3}	1.06×10^{-2}
9	3.01×10^{-5}	1.59×10^{-8}	1.83×10^{-3}	6.53×10^{-3}
10	1.83×10^{-5}	6.75×10^{-9}	1.08×10^{-3}	4.27×10^{-3}

TABLE 2. Convergence results for a single axon setting $\tau = 0.001\exp(-\frac{K}{2}+1)$ in order to keep the relation $\tau \propto \exp(-K)$. The rates of exponential convergence are 1.9114, 0.5486 and 0.4534 for the single, two and three cell cases, respectively.

Simulations are carried out assuming a membrane behavior given by the HH model [26, 17]. Besides, in the computations presented here, we consider the following external source

$$\Phi_e(\boldsymbol{x}) = -\mathbf{E}\cdot\boldsymbol{x}, \tag{7.1}$$

which represents the potential produced by an electric field $\mathbf{E}$. The electric field $\mathbf{E}$ is assumed to be constant in space and time. The error is measured in the following norm

$$\|\boldsymbol{u}\|_{L^\infty(\Upsilon_N,\mathbb{L}^2_J)} := \max_{t_n\in\Upsilon_N} \|\boldsymbol{u}(t_n)\|_{\mathbb{L}^2_J}\,. \tag{7.2}$$

7.1. **Convergence Results.** We present convergence results of the numerical scheme presented in Section 6. We consider three different configurations, as depicted in Figure 1. Figures 1i, 1ii and 1iii show one, two and three biological cell configurations, respectively. Convergence analysis is performed with a number of Fourier modes K ranging from 1 up to 10 and time steps are chosen such that $\tau \propto \exp(-\frac{K}{2})$ for the simulation time window $[0,1]$ ms.

Table 2 shows convergence results for the configurations described in Figures (1i), (1ii) and (1iii) assuming $d = 0.1R$ and $\mathbf{E} = (5000,0,0)^\top$ mV/cm. The first column in Table 2 is the number of Fourier modes K, the second column corresponds to the time step τ, which has been chosen according to the rule $\tau = 0.001\exp(-\frac{K}{2}+1)$. Finally, the third, fourth and fifth columns present the error measured in the $\|\cdot\|_{L^\infty(\Upsilon_N,\mathbb{L}^2_J)}$–norm as defined in (7.2), with $J = 1,2,3$, for the single, two and three biological cells configurations presented in Figure 1, respectively.

7.2. **Transmembrane Voltage.** We now present the profile of transmembrane voltages at different points over the biological cell for the three configurations described in Figure 1. Figure 2 shows the transmembrane voltage for the single biological cell configuration at points (a) and (b) defined in Figure 1i. The electric field employed in this computation is $\mathbf{E} = (5000,0,0)^\top$ mV/cm. Figures 3 – 6 shown results for the two cells

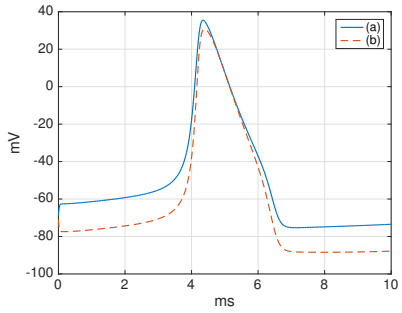

FIGURE 2. Transmembrane potential of the single biological cell setting at points (a) and (b) as defined in Figure (1i). The electric field used in this computation is $\mathbf{E} = (5000, 0, 0)^\top$ mV/cm.

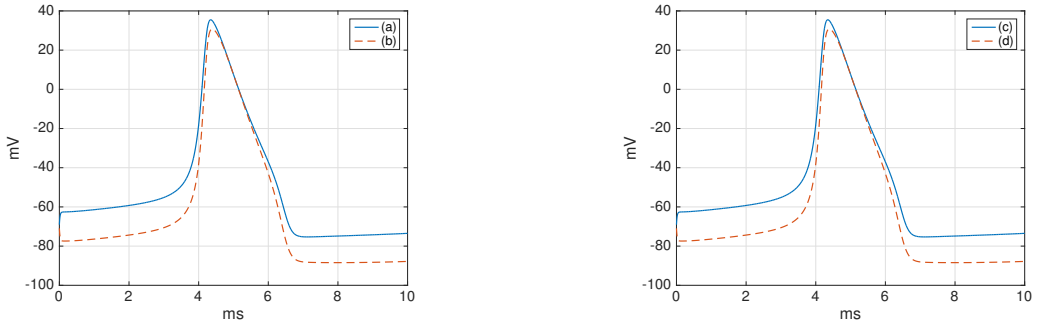

(i) (ii)

FIGURE 3. Transmembrane potential of the two biological cells setting. The electric field is this computation is $\mathbf{E} = (5000, 0, 0)^\top$ mV/cm and the distance between cells is $d = 5R$. Figure 6i portrays the transmembrane voltage at points (a) and (b) and Figure 6ii at points (c) and (d), as defined in Figure 1ii.

scenario. In Figure 3 the distance between cells is $d = 5R$ and the electric field is $\mathbf{E} = (5000, 0, 0)^\top$ mV/cm. In Figure 4 the electric field remains the same, however the distance between cells is reduced to $d = 0.1R$. In Figures 5 and (6) the distance between cells is still $d = 0.1R$, nevertheless the electric field is increased to $\mathbf{E} = (6000, 0, 0)^\top$ mV/cm and $\mathbf{E} = (7500, 0, 0)^\top$ mV/cm, respectively. Figures 7 and 8 portray the results for the three biological configuration, presented in Figure 1iii. In both figures, the distance between biological cells is $d = 0.1R$ however in the Figure 7 the electric field is $\mathbf{E} = (5000, 0, 0)^\top$ mV/cm, while in Figure 8 it is set to $\mathbf{E} = (7500, 0, 0)^\top$ mV/cm.

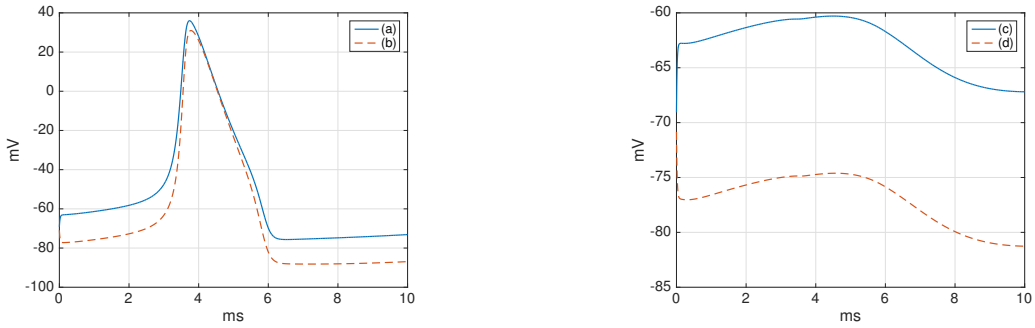

(i) (ii)

FIGURE 4. Transmembrane potential of the two biological cells setting. The electric field used int this computation is $\mathbf{E} = (5000, 0, 0)^\top$ mV/cm and the distance between cells is $d = 0.1R$. Figure 6i portrays the transmembrane voltage at points (a) and (b) and Figure 6ii at points (c) and (d), as defined in Figure 1ii.

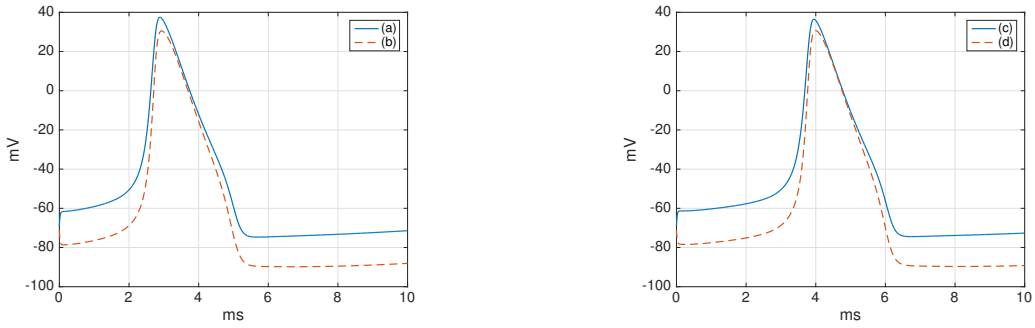

(i) (ii)

FIGURE 5. Transmembrane potential of the two biological cells setting. The electric field is this computation is $\mathbf{E} = (6000, 0, 0)^\top$ mV/cm and the distance between cells is $d = 0.1R$. Figure 6i portrays the transmembrane voltage at points (a) and (b) and Figure 6ii at points (c) and (d), as defined in Figure (1ii).

We now present results for the electrical interaction of 25 biological cells distributed in a homogeneous lattice of size 5×5, as shown in Figure 9. Cells are numbered following the scheme presented in Figure 9i. As in previous computations, all the cells are of equal radius R with a distance between them is $d = 0.2R$, as portrayed in Figure 10. Figure for 9 out the 25 biological cells we have considered in the computation. The transmembrane potential at the left and rightmost points, respectively points (a) and (b) as described in Figure 10, are plotted. Figures 10i–10iii show results for the biological cells in positions 1×1, 1×3 and 1×5. Figures 10iv–10vi show results for the biological cells in positions 3×1, 3×3 and 3×5. Figures 10vii–10ix show results for the biological cells in positions 5×1, 5×3 and 5×5.

7.3. **Discussion.** The results validate the expected exponential convergence rates of when taking $\tau \propto \exp(-K/2)$ for both linear and nonlinear membrane dynamics. Based on this observation, we calibrate our quadrature scheme for the nonlinear terms using the same spatial nodes. Indeed, higher order quadratures would not improve convergence rates though perhaps proportionality constants. In terms of computational effort, we observe a rapid increase in computational times as expected as no acceleration routines were implemented. Interestingly, we observed that as cells came closer to each other exponential rates decreased. This can be explained by a loss of analyticity in the solutions, which disappears once cells touch each other.

From a biological perspective, our numerical results support the claim for membrane potentials depending on both axon geometry and position with respect to external electrical excitations. Such interrelations are

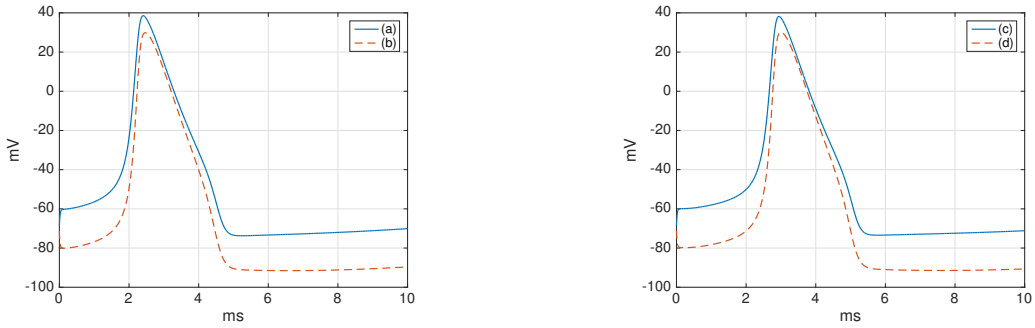

(i) (ii)

FIGURE 6. Transmembrane potential of the two biological cells setting. The electric field is this computation is $\mathbf{E} = (7500, 0, 0)^\top$ mV/cm and the distance between cells is $d = 0.1R$. Figure 6i portrays the transmembrane voltage at points (a) and (b) and Figure 6ii at points (c) and (d), as defined in Figure (1ii).

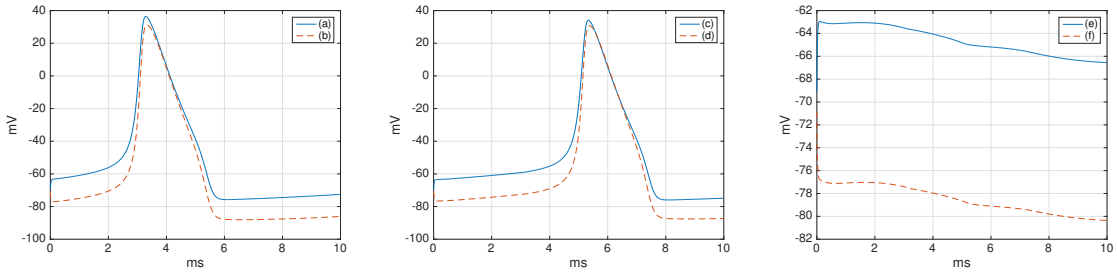

(i) (ii) (iii)

FIGURE 7. Transmembrane potential of the three biological cells setting. The electric field is this computation is $\mathbf{E} = (5000, 0, 0)^\top$ mV/cm and the distance between cells is $d = 0.1R$. Figure (7i) portrays the transmembrane voltage at points (a) and (b); Figure (7ii) at points (c) and (d); and Figure (7iii) at points (e) and (f), as defined in Figure (1iii).

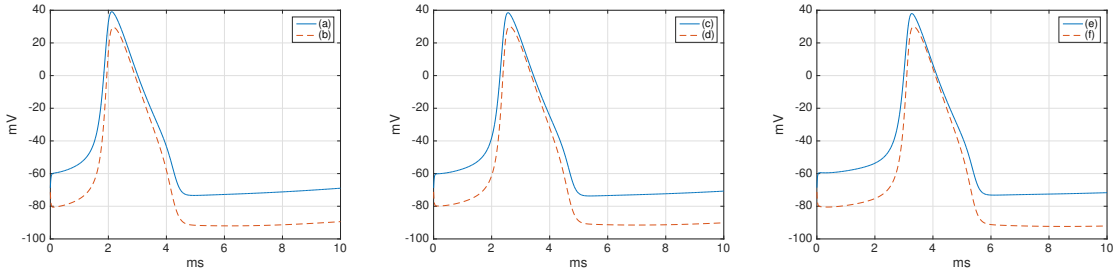

(i) (ii) (iii)

FIGURE 8. Transmembrane potential of the three biological cells setting. The electric field is this computation is $\mathbf{E} = (7500, 0, 0)^\top$ mV/cm and the distance between cells is $d = 0.1R$. Figure (8i) portrays the transmembrane voltage at points (a) and (b); Figure (8ii) at points (c) and (d); and Figure (8iii) at points (e) and (f), as defined in Figure (1iii).

extremely relevant when analyzing and modeling closely packed cells and their interactions [39]. For instance, cells lying between the excitation and a given target cell can delay or even block the stimulation.

Furthermore, our model is capable of portraying oscillatory behavior under pre-polarization regime for sinusoidal external excitations. As in the case of constant fields, there exists a jump in main voltage when

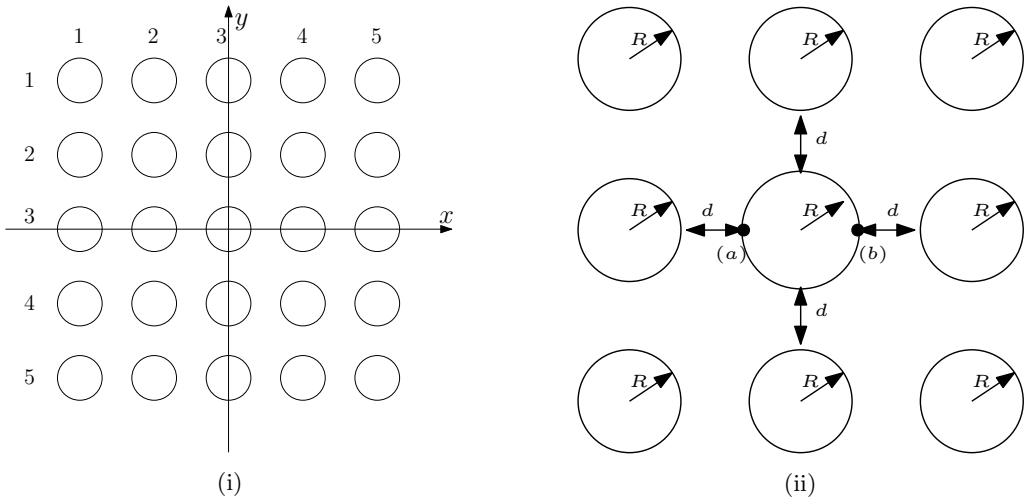

FIGURE 9. Configuration of 25 interacting biological cells. The cells are arranged in a grid of size 5×5 as depicted in Figure 9i. The distance between cells is $d = 0.2R$ and transmembrane voltage is measured at points and (a) and b, as depicted in 10.

threshold values are achieved for a sufficient periods. Interestingly, when increasing the excitation frequency thresholds are achieved sooner in agreement with experimental results [10, 8, 42]. Numerically, the method remains stable when considering with time-varying excitations but careful attention should be given to sampling rates of the sources applied.

8. Conclusions and Future Work

We have presented a novel numerical method to compute the temporal evolution of cellular membrane potentials under electrical excitation. Key to the success of the scheme is the boundary reduction via the MTF along with the coupling of the Hodgin-Huxley model for transmembrane voltages. The resulting problem is proven to be well posed via analytic semigroup theory. In time-domain, the proposed semi-implicit method was shown to possess a time-step stability condition independent of the spatial discretization, relying solely on problem parameters. Moreover, for analytic solutions exponential convergence rates were found for suitable chosen time and space steps, which was validated numerically for two-dimensional cells. Simulations are found to agree with experimental observations. In particular, our numerical results depict the blocking effect that surrounding axons can yield onto a particular one as well as the change of excitation phase due to the multiple cellular interactions. Future work includes the extension to 3D simulations as well as further acceleration for cross interactions including the use iterative solvers by implementing preconditioners based on Calderón identities or mass matrices.

References

[1] M. Amar, D. Andreucci, P. Bisegna, R. Gianni, et al. A hierarchy of models for the electrical conduction in biological tissues via two-scale convergence: the nonlinear case. *Differential and Integral Equations*, 26(9/10):885–912, 2013.

[2] M. Amar, D. Andreucci, and R. Gianni. Asymptotic decay under nonlinear and noncoercive dissipative effects for electrical conduction in biological tissues. *Nonlinear Differential Equations and Applications NoDEA*, 23(4):48, 2016.

[3] E. Anderson, Z. Bai, C. Bischof, S. Blackford, J. Dongarra, J. Du Croz, A. Greenbaum, S. Hammarling, A. McKenney, and D. Sorensen. *LAPACK Users' guide*, volume 9. SIAM, 1999.

[4] X. Antoine, C. Chniti, and K. Ramdani. On the numerical approximation of high-frequency acoustic multiple scattering problems by circular cylinders. *Journal of Computational Physics*, 227(3):1754–1771, 2008.

[5] K. Atkinson and W. Han. *Theoretical numerical analysis*, volume 39. Springer, 2005.

[6] M. Balabane. Boundary decomposition for helmholtz and maxwell equations 1: disjoint sub-scatterers. *Asymptotic Analysis*, 38(1):1–10, 2004.

[7] P. J. Basser and B. J. Roth. New currents in electrical stimulation of excitable tissues. *Annual review of biomedical engineering*, 2:377–397, 2000.

[8] N. Bhadra, E.A. Lahowetz, S.T. Foldes, and K.L. Kilgore. Simulation of high-frequency sinusoidal electrical block of mammalian myelinated axons. *Journal of Computational Neuroscience*, 22(3):313–326, 2007.

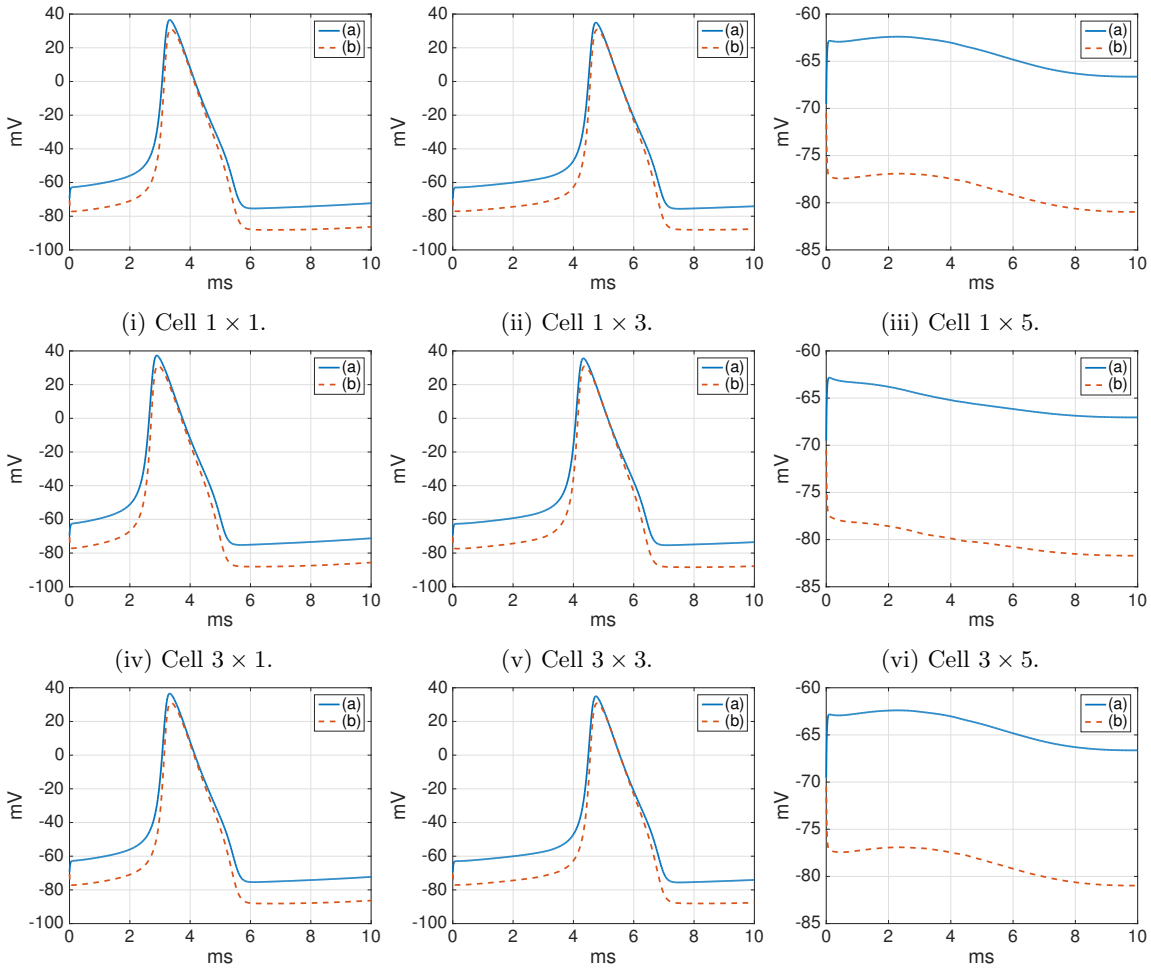

(i) Cell 1×1. (ii) Cell 1×3. (iii) Cell 1×5.

(iv) Cell 3×1. (v) Cell 3×3. (vi) Cell 3×5.

(vii) Cell 5×1. (viii) Cell 5×3. (ix) Cell 5×5.

FIGURE 10. Transmembrane potential in the 5×5 biological cells configuration shown Figure 9. The electric field is this computation is $\mathbf{E} = (7500, 0, 0)^\top$ mV/cm. We show the transmembrane potential at points (a) and (b) as described in Figure , i.e. the left and rightmost points on the boundary of the biological cell. We show results for 9 of the 25 biological cells, following the numbering described in Figure 9i.

[9] C. Bollini and F. Cacheiro. Peripheral nerve stimulation. *Techniques in Regional Anesthesia and Pain Management*, 10(3):79–88, 2006.

[10] B.R. Bowman and D.R. McNeal. Response of single alpha motoneurons to high-frequency pulse trains. firing behavior and conduction block phenomenon. *Applied neurophysiology*, 49(3):121–138, 1986.

[11] C. Canuto and A. Quarteroni. Approximation results for orthogonal polynomials in sobolev spaces. *Mathematics of Computation*, 38(157):67–86, 1982.

[12] Claudio Canuto, M Yousuff Hussaini, Alfio Quarteroni, and Thomas A Zang. Spectral methods. scientific computation. In *Fundamentals in Single Domains*. Springer-Verlag Berlin, 2006.

[13] S. O. Choi, Y.C. Kim, J. W. Lee, J. H. Park, M. R. Prausnitz, and M. G. Allen. Intracellular protein delivery and gene transfection by electroporation using a microneedle electrode array. *Small*, 10(8):1081–1091, 2012.

[14] X. Claeys, R. Hiptmair, and C. Jerez-Hanckes. Multitrace boundary integral equations. In *Direct and inverse problems in wave propagation and applications*, volume 14 of *Radon Ser. Comput. Appl. Math.*, pages 51–100. De Gruyter, Berlin, 2013.

[15] X. Claeys, R. Hiptmair, C. Jerez-Hanckes, and S. Pintarelli. Novel multi-trace boundary integral equations for transmission boundary value problems. In A. S. Fokas and B. Pelloni, editors, *Unified Transform for Boundary Value Problems: Applications and Advances*, chapter Novel Multi-Trace Boundary Integral Equations for Transmission Boundary Value Problems. SIAM, 2015.

[16] M. Costabel. Boundary integral operators on lipschitz domains: elementary results. *SIAM J. Math. Anal.*, 19(3):613–626, 1988.

[17] S. Doi, J. Inoue., Z. Pan, and K. Tsumoto. *Computational Electrophysiology*, volume 2. Tokyo, Japan: Springer Series, A First Course in On Silico Medicine, 2010.

[18] I. Dotsinskya, B. Nikolovaa, E. Peychevab, and I. Tsonevaa. New modality for electrochemotherapy of surface tumors. *Biotechnology & Biotechnological Equipment*, 26(6):3402–3406, 2012.

[19] M. Ganesh and S. C. Hawkins. A high-order algorithm for multiple electromagnetic scattering in three dimensions. *Numerical Algorithms*, 50(4):469–510, 2009.

[20] M. Ganesh and S.C. Hawkins. Simulation of acoustic scattering by multiple obstacles in three dimensions. *ANZIAM Journal*, 50:31–45, 2008.

[21] M. Ganesh and S.C. Hawkins. An efficient\ mathcal {O}(n) algorithm for computing\ mathcal {O}(nˆ 2) acoustic wave interactions in large n-obstacle three dimensional configurations. *BIT Numerical Mathematics*, 55(1):117–139, 2015.

[22] M. Ganesh and K. Mustapha. A fully discrete h^1-galerkin method with quadrature for nonlinear advection–diffusion–reaction equations. *Numerical Algorithms*, 43(4):355–383, 2006.

[23] D. Gottlieb and S.A. Orszag. *Numerical analysis of spectral methods: theory and applications*. Society for Industrial and Applied Mathematics, 1983.

[24] F. Henríquez, C. Jerez-Hanckes, and F. Altermatt. Boundary integral formulation and semi-implicit scheme coupling for modeling cells under electrical stimulation. *Numerische Mathematik*, 136(1):101–145, 2016.

[25] R. Hiptmair and C. Jerez-Hanckes. Multiple traces boundary integral formulation for helmholtz transmission problems. *Advances in Computational Mathematics*, 37(1):39–91, 2012.

[26] A.L. Hodgkin and A.F. Huxley. A quantitative description of membrane current and its application to conduction and excitation in nerve. *The Journal of Physiology*, 117(4):500–544, 1952.

[27] S. Joucla and B. Yvert. Modeling extracellular electrical neural stimulation: From basic understanding to mea-based applications. *Journal of Physiology, Paris*, 106(3):146–158, 2011.

[28] Sébastien Joucla, Alain Glière, and Blaise Yvert. Current approaches to model extracellular electrical neural microstimulation. *Frontiers in computational neuroscience*, 8:13, Feb 2014.

[29] J. Keener and J. Sneyd. *Mathematical Physiology I: Cellular Physiology*. Springer-Verlag, New York, 1998.

[30] R. Kress. *Linear integral equations*, volume 82. Springer, 1989.

[31] R. Kress and I. H Sloan. On the numerical solution of a logarithmic integral equation of the first kind for the helmholtz equation. *Numerische Mathematik*, 66(1):199–214, 1993.

[32] K. Lindsay. From maxwell's equations to the cable equation and beyond. *Progress in Biophysics and Molecular Biology*, 85(1):71–116, 2004.

[33] A. Lunardi. *Analytic semigroups and optimal regularity in parabolic problems*. Springer Science & Business Media, 2012.

[34] Philip K. Maini. Making sense of complex phenomena in biology. *Novartis Foundation symposium*, 247:53–9; discussion 60–5, 84–90, 244–52, 2002.

[35] P.A. Martin. *Multiple scattering: interaction of time-harmonic waves with N obstacles*. Cambridge University Press, 2006.

[36] H. Matano and Y. Mori. Global existence and uniqueness of a three-dimensional model of cellular electrophysiology. *Discrete Contin. Dyn. Syst*, 29:1573–1636, 2011.

[37] William McLean. *Strongly elliptic systems and boundary integral equations*. Cambridge University Press, Cambridge, 2000.

[38] L. M. Mir, M. F. Bureau, J. Gehl, R. Rangara, D. Rouy, J. M. Caillaud, P. Delaere, D. Branellec, B. Schwartz, and D. Scherman. High-efficiency gene transfer into skeletal muscle mediated by electric pulses. *Proc. Nat. Acad. Sci. USA.*, 96(8):4262–4267, 1999.

[39] M. Pavlin, N. Pavselj, and D. Miklavcic. Dependence of induced transmembrane potential on cell density, arrangement and cell position inside a cell system. *IEEE Transactions on Biomedical Engineering.*, 40(6):605–612, 2002.

[40] Amnon Pazy. *Semigroups of linear operators and applications to partial differential equations*, volume 44. Springer Science & Business Media, 2012.

[41] C. Pham-Dang, O. Kick, T. Collet, F. Gouin, and M. Pinaud. Continuous peripheral nerve blocks with stimulating catheters. *Regional Anesthesia and Pain Medicine*, 28(2):83–88, 2003.

[42] F. Rattay. High frequency electrostimulation of excitable cells. *Journal of Theoretical Biology*, 123(1):45–45, 1986.

[43] T. Runst and W. Sickel. *Sobolev spaces of fractional order, Nemytskij operators, and nonlinear partial differential equations*, volume 3. Walter de Gruyter, 1996.

[44] J. Saranen and G. Vainikko. *Periodic integral and pseudodifferential equations with numerical approximation*. Springer Science & Business Media, 2013.

[45] S. Sauter and C. Schwab. *Boundary Element Methods*. Springer-Verlag, Berlin Heidelberg, 2011.

[46] N. Sepulveda, J. Wikswo, and D. Echt. Finite element analysis of cardiac defibrillation current distributions. *EEE Transactions on Biomedical Engineering*, 37(4):354–365, 1997.

[47] G. Sersa, T. Cufer, M. Cemazar, M. Rebersek, and R. Zvonimir. Electrochemotherapy with bleomycin in the treatment of hypernephroma metastasis: case repeat and literature review. *Tumori*, 86(2):163–165, 2000.

[48] O. Steinbach. *Numerical approximation methods for elliptic boundary value problems*. Springer–Verlag, New York, 2008.

[49] Eitan Tadmor. The exponential accuracy of fourier and chebyshev differencing methods. *SIAM Journal on Numerical Analysis*, 23(1):1–10, 1986.

[50] J. Teissié, N. Eynard, B. Gabriel, and M.P. Rols. Electropermeabilization of cell membranes. *Adv. Drug. Del. Rev*, 35(1):3–19, 1999.

[51] V. Thomée. *Galerkin Finite Element Methods for Parabolic Problems*. Springer Series in Computational Mathematics, 2006.
[52] N. Trayanova, J. Constantino, T. Ashihara, and G. Plank. Modeling defibrillation of the heart: Approaches and insights. *IEEE Reviews in Biomedical Engineering*, 4:89–102, 2012.
[53] U. van Rienen, U. Schreiber, S. Schulze, U.Gimsa, W. Baumann, D.G. Weiss, J. Gimsa, R. Benecke, and H.W. Pau. Electro-quasistatic simulations in bio-systems engineering and medical engineering. *Advances in Radio Science*, 3:39–49, 2005.
[54] P.C. Waterman. Matrix formulation of electromagnetic scattering. *Proceedings of the IEEE*, 53(8):805–812, 1965.

Seminar for Applied Mathematics, ETH Zürich, CH-8092 Zürich, Switzerland
E-mail address: fernando.henriquez@sam.math.ethz.ch

School of Engineering, Pontificia Universidad Católica de Chile, Santiago, Chile
E-mail address: cjerez@ing.puc.cl